

Inspecting differences between multivariate distributions: graphical tool-kit and related tests

Pratim Guha Niyogi

Johns Hopkins University

Department of Biostatistics

Baltimore, MD 21205, USA

Email ID: pnyogi1@jhmi.edu

Subhra Sankar Dhar

IIT Kanpur

Department of Mathematics and Statistics

Kanpur 208106, India

Email ID: subhra@iitk.ac.in

January 5, 2023

Abstract

This article inspects whether a multivariate distribution is different from a specified distribution or not, and it also tests the equality of two multivariate distributions. In the course of this study, a graphical tool-kit based on well-known half-spaced depth is proposed, which is a two-dimensional plot, regardless of the dimension of the data, and it is even useful in comparing high-dimensional distributions. The simple interpretability of the proposed graphical tool-kit motivates us to formulate test statistics to carry out the corresponding testing of hypothesis problems. It is established that the proposed tests are consistent, and moreover, the asymptotic distributions of the test statistics under contiguous alternatives are derived, which enable us to compute the asymptotic power of these tests. Furthermore, it is observed that the computations associated with the proposed tests are unburdensome. Besides, these tests perform better than many other tests available in the literature when data are generated from various distributions such as heavy tailed distributions, which indicates that the proposed methodology is robust as well. Finally, the usefulness of the proposed graphical tool-kit and tests is shown on two benchmark real data sets.

Key words and phrases: goodness-of-fit test; two-sample test; half-space depth; data-depth plot; hypothesis testing

1 Introduction

In many scientific investigations, data are collected for multiple variables, and therefore, some techniques are needed to visualize and compare multivariate observations. In this spirit, this article addresses the problem of goodness-of-fit to validate the assumption of the underlying multivariate distribution, which is commonly encountered in many statistical data analyses. Moreover, we propose statistical tests to compare two multivariate probability distributions along with appropriate graphical tool-kits. It is needless to mention that such testing of hypothesis problems have a plethora of applications. For example, to understand the dynamics of the human physical activity patterns, the distribution of diurnal activity and the rest period is assumed to be a double Pareto distribution, and in order to validate it, a goodness-of-fit test is needed (Paraschiv-Ionescu et al., 2013). In psychology, the study of maternal depression, examination of maternal and infant sleep throughout the first year of life is an example of a two-sample testing problem (Newland et al., 2016).

Let us now formulate the problem with notation. Consider the data $\mathcal{X} = \{\mathbf{X}_1, \dots, \mathbf{X}_n\}$ associated with unknown distribution F , and F_0 is the specified distribution function on \mathbb{R}^d ($d \geq 1$). We now want to test that $H_0 : F = F_0$ against $H_1 : F \neq F_0$, and a few more technical assumptions on F and F_0 will be stated at appropriate places. Moreover, as said before, the two-sample problem for comparing multivariate distributions can also be formulated in the following way. Suppose that $\mathcal{X} = \{\mathbf{X}_1, \dots, \mathbf{X}_n\}$ and $\mathcal{Y} = \{\mathbf{Y}_1, \dots, \mathbf{Y}_m\}$ are two independent data sets associated with two unknown multivariate distributions F and G , respectively. Here, we now want to test $H_0 : F = G$ against $H_1 : F \neq G$. For $d = 1$, i.e., in the case of univariate data, the aforesaid problems have already been investigated in many articles. For example, the readers may refer to Kolmogorov-Smirnov (KS) (Daniel, 1990), Cramér-von Mises (CvM) (Anderson, 1962), Anderson-Darling (AD) (Anderson and Darling, 1952) and few more tests. In this context, for comparing univariate distributions, we would like to mention that a few graphical tool-kits have also been used in literature for a long time such as probability-probability plot (Michael, 1983) quantile-quantile plot (Gnanadesikan, 2011; Wilk and Gnanadesikan, 1968; Chambers et al., 2018), Lorenz curve (Lorenz, 1905).

For $d > 1$, such statistical tests have been studied like AD test (Paulson et al., 1987), CvM test (Koziol, 1982), Doornik-Hansen (DH) test (Doornik and Hansen, 2008), Henze-Zirkler (HZ) test (Henze and Zirkler, 1990), Royston (R) test (Roys-

ton, 1992) and a series of χ^2 -type tests (for example McCulloch (M), Nikulin-Rao-Robson (NRR), Dzhaparidze-Nikulin (DN) (Voinov et al., 2016)). These tests validate whether the data are obtained from multivariate normality assumption or not. For two-sample multivariate problems, similar studies have been investigated by Chen and Friedman (2017) and see a few references therein. Besides, like univariate data, there have been a few attempts in visualizing two multivariate distributions in two-dimensional plots (see for example, Friedman and Rafsky (1981); Marden (1998, 2004); Dhar et al. (2014)). However, none of the above tests and graphical toolkits are easily implementable to large-dimensional data.

To overcome aforesaid difficulties, we introduce two test statistics based on the difference of some functions that are equipped to measure the closeness of an arbitrary point in a space located to an implicitly defined center of the data (Tukey, 1975). This function is known as data-depth (for details see Liu et al. (1999)), and the proposed test procedure is called data-depth discrepancy (DDD). Here, DDD is large for the majority of the sample points if and only if, the assumption on the parent distribution is likely wrong (in goodness-of-fit test) or the samples are likely from different distributions (in two-sample test). In this work, DDD is defined based on L_2 and L_∞ distance between two relevant data-depth functions which provide us corresponding KS and CvM test statistics. However, to measure DDD, one may use other suitable distance functions (such as $L_p, p \geq 1$ distance) in principle. The well-known concept of data-depth for multivariate data is briefly reviewed next.

To study various features of multivariate distribution, there are some usual extensions of the moment-based approach in univariate setup, and exemplary three such features are location, scale, and shape. It is well-known that these features can be captured by different moments and their certain functions, if the moments exist. Even for univariate data, one can employ the concept of the rank of the observations instead of moments to study those features associated with descriptive statistics. However, the concept of the rank is not uniquely defined for multivariate data unlike the univariate data. Data-depth is a general extension of the standard univariate rank of the distribution that is easy to plot on a plane, and therefore easy to visualize (Liu et al., 1999). Although the rank in the univariate case assigns a ‘linear ranking’ from the smallest to the largest data point, depth is a measure of ‘center-outward’ ranking, which starts from middle sample points and increases outward in all directions. The highest depth is associated with the deepest or central point, and the smallest depth corresponds to the most outlying point with respect to the data cloud. There are

various types of data-depths that include Mahalanobis depth (Mahalanobis, 1936) and spatial depth (Gower, 1974; Brown and Hettmansperger, 1989) based on the two moments, half-space depth (Hodges, 1955; Tukey, 1975) based on the geometry of the half-spaces among many others. For an overview on various depth functions, we refer to Zuo and Serfling (2000) and the references therein.

In this article, we propose DDD based on Tukey's half-space depth since it uniquely determines a uniformly absolutely continuous distribution with compact support under minimal assumptions (Koshevoy, 2002; Hassairi and Regaieg, 2008). In addition, this can be easily computed since there exist some packages that are freely available in various statistical softwares such as R. In order to carry out the test, we replace the distribution function with data-depth and propose KS and CvM type test statistics for the goodness-fit and the two-sample tests. Along with the construction of the aforesaid tests, following are the main contributions of this article. First, we define a discrepancy measure based on half-space depth, which can be used to create an alternative graphical tool-kit to visualize the disparity of two distribution functions. Second, we propose two test statistics based on the proposed discrepancy measure for both goodness-of-fit and two-sample testing procedures. Third, most of the existing test statistics are available for the normality test only; our testing procedure provides a computationally feasible unified solution for any underlying distribution for any dimension. Fourth, we have shown that the proposed tests are consistent. Moreover, the asymptotic distributions of the test statistics under the contiguous alternative are derived, which enables us to compute the asymptotic power of the tests under contiguous alternatives. Fifth, a new graphical tool-kit based on discrepancy measure is introduced here. The diagram related to our proposed graphical tool-kit lies on the two-dimensional plane irrespective of the dimension of the data. This fact enables us to visualize features of fairly large-dimensional data using the proposed graphical tool-kit.

The rest of the paper is organized as follows. In Section 2, we briefly review the different well-known notions of data-depth, usefulness of Tukey's half-space depth and a graphical display, called depth-depth plot. Section 3 is dedicated to the proposed methods in statistical testing for goodness-of-fit and two-sample situations. First, we provide the heuristic establishment of the graphical tool-kit, and in later part of Section 3, we proceed with the formal definition of DDD and conclude with two multivariate tests based on the data-depth. In Section 4, we investigate the asymptotic properties of the proposed testing procedures. The finite sample performance is

presented in Section 5. Finally, in Section 6, we implement the proposed test on two interesting data sets. Section 7 concludes the article with a discussion. At the end, Appendix contains all technical details and mathematical proofs.

The codes of all numerical studies are made available at <https://github.com/pratimguhaniyogi>.

2 Some preliminaries

In the pioneering work by John W. Tukey in 1975, he introduced a novel way to describe the data cloud. For a given multivariate data cloud $\mathcal{X} = \{\mathbf{X}_1, \dots, \mathbf{X}_n\}$, a point \mathbf{x} in the same Euclidean space becomes the representative of \mathcal{X} through the function $D_{\mathcal{X}}(\mathbf{x})$, which measures how ‘close’ \mathbf{x} is to the center of \mathcal{X} . Mathematically, a function, viz., depth function, will be bounded non-negative function of the form $D : \mathbb{R}^d \times \mathcal{F} \rightarrow \mathbb{R}$ where \mathcal{F} is the class of all distributions on \mathbb{R}^d . In most of the examples of the data-depth, the functions are affine invariant in the scenes $D_{F_{\mathbf{Ax}+\mathbf{b}}}(\mathbf{Ax} + \mathbf{b}) = D_{F_{\mathbf{x}}}(\mathbf{x})$ for any $d \times d$ matrix \mathbf{A} and a vector $\mathbf{b} \in \mathbb{R}^d$ and a quasi-concave function that maximizes somewhere in the center of the data cloud and vanishes to infinity. Many data-depth functions are proposed such as Mahalanobis (Mahalanobis, 1936), half-space depth (Tukey, 1975), simplicial volume (Oja, 1983), simplicial (Liu, 1990), projection (Zuo and Serfling, 2000) etc. Mosler (2013) provides a detailed survey of such depth measures with their properties.

Half-space depth is one of the depth functions which does not impose any moment conditions of the data, and can be computed nonparametrically and can characterize certain family of distributions (Koshevoy, 2003; Hassairi and Regaieg, 2008; Cuesta-Albertos and Nieto-Reyes, 2008; Kong and Zuo, 2010). The technical definition of the half-space depth is as follows. Let F be a probability distribution on \mathbb{R}^d for $d \geq 1$ and \mathcal{H} be the class of closed half-spaces H in \mathbb{R}^d . The Tukey’s depth (or half-space depth) of a point $\mathbf{x} \in \mathbb{R}^d$ with respect to F is defined by

$$D_F(\mathbf{x}) = \inf \{F(H) : H \in \mathcal{H}, \mathbf{x} \in H\}. \quad (1)$$

One may also look at $D_F(\cdot)$ in the following way. Let $\mathcal{S}^{d-1} = \{\mathbf{u} \in \mathbb{R}^d : \|\mathbf{u}\| = 1\}$ be the unit sphere of \mathbb{R}^d , then for $\mathbf{u} \in \mathcal{S}^{d-1}$ and $\mathbf{x} \in \mathbb{R}^d$, we consider the closed half-space $H[\mathbf{x}, \mathbf{u}] = \{\mathbf{y} \in \mathbb{R}^d : \mathbf{u}^T \mathbf{x} \geq \mathbf{u}^T \mathbf{y}\}$. Now, the Tukey’s half-space depth with

respect to the distribution function F can be defined as

$$D_F(\mathbf{x}) = \inf_{\mathbf{u} \in \mathcal{S}^{d-1}} F(H[\mathbf{x}, \mathbf{u}]). \quad (2)$$

The sample version of $D_F(\mathbf{x})$, which is denoted as $D_{\mathcal{X}}(\mathbf{x})$, based on the empirical distribution \widehat{F}_n of the sample $\mathcal{X} = \{\mathbf{X}_1, \dots, \mathbf{X}_n\}$ and is defined as

$$D_{\mathcal{X}}(\mathbf{x}) = \min_{\mathbf{u} \in \mathcal{S}^{d-1}} \frac{1}{n} \sum_{i=1}^n \mathbf{1}\{\mathbf{X}_i^T \mathbf{u} \leq \mathbf{x}^T \mathbf{u}\}. \quad (3)$$

Observe that, for $d = 1$, $D_F(x) = \min\{F(x), S(x)\}$, where $S(x) = 1 - F(x)$. Since $\widehat{F}_n(x)$ is the right-continuous empirical cumulative distribution function, we define $\widehat{S}_n(x) = 1 - \widehat{F}_n(x^-)$, and consequently, the sample version of half-space depth for univariate data becomes $D_{\mathcal{X}}(x) = \min\{\widehat{F}_n(x), \widehat{S}_n(x)\}$. Based on this definition, it can easily be observed that the depth function achieves the maximum at the median of the distribution and monotonically decays to zero when x deviates from the median. Massé (2004) provided some results on asymptotics for the half-space depth process, and Rousseeuw and Ruts (1996); Ruts and Rousseeuw (1996); Rousseeuw and Struyf (1998) pointed out the computational aspects of the half-space depth.

As a graphical tool-kit, the depth-depth (DD) plot (Liu et al., 1999) is an important tool to compare two multivariate distributions graphically. For the sake of completeness, we here briefly describe the methodology of the DD-plot. We plot the depth values of the combined sample under the two corresponding empirical distributions. Let F and G be two distributions on \mathbb{R}^d , and let $D(\cdot)$ be an affine-invariant depth (for example, half-space depth). Define the population version of DD-plot,

$$DD(F, G) = \{(D_F(\mathbf{x}), D_G(\mathbf{x})) \text{ for all } \mathbf{x} \in \mathbb{R}^d\}. \quad (4)$$

If the two distributions are identical, then these graphs are segments of the diagonal line from $(0,0)$ to $(1,1)$ on the \mathbb{R}^2 plane. Plots that deviate from the straight line indicate the difference of two underlying distributions. For goodness-of-fit problem, if the underlying distribution F is unknown, for a given sample $\{\mathbf{X}_1, \dots, \mathbf{X}_n\}$, we may determine whether F is some specified distribution, say G , by examining the sample version of DD-plot

$$DD(\mathcal{X}, G) = \{(D_{F_n}(\mathbf{x}), D_G(\mathbf{x})) \text{ for all } \mathbf{x} \in \{\mathbf{X}_1, \dots, \mathbf{X}_n\}\}. \quad (5)$$

For two-sample problem, if F and G are the population distributions for the sample $\mathcal{X} = \{\mathbf{X}_1, \dots, \mathbf{X}_n\}$ and $\mathcal{Y} = \{\mathbf{Y}_1, \dots, \mathbf{Y}_m\}$, respectively, one can use the DD-plot to determine whether or not the two distributions are identical.

$$DD(\widehat{F}_n, \widehat{G}_m) = \{(D_{\widehat{F}_n}(\mathbf{x}), D_{\widehat{G}_m}(\mathbf{x})) \text{ for all } \mathbf{x} \in \{\mathcal{X} \cup \mathcal{Y}\}\}. \quad (6)$$

It is easy to check that the DD-plot is affine-invariant if the associated depth measures are so be. On the one hand, if $d = 1$, the Lebesgue measure of DD vanishes when $F \neq G$, and on the other hand, for $d > 1$ and F and G are absolutely continuous, DD is a region with non-zero area. Moreover, Liu et al. (1999) showed that, for different distributional differences, such as location, scale, skewness, and kurtosis, different patterns are observed in the DD-plot.

3 Data-depth discrepancy and associated tests

In this section, we propose a data-depth discrepancy (DDD) describing a graphical tool-kit and associated tests. The DDD is defined in terms of the difference of the depth functions, and we begin this discussion in Section 3.1 for any probability distribution. We conclude this section with the motivation for defining a graphical tool-kit to visualize the dissimilarities of the distributions. We introduce new multivariate goodness-of-fit and two-sample tests based on half-space depth in Section 3.2.

3.1 Data-depth discrepancy (DDD)

Our goal is to construct statistical tests that can answer the following questions.

Problem 1. (One-sample/Goodness-of-fit multivariate problem) For $d \geq 1$, let \mathbf{X} be a d -dimensional random variable with distribution function F on \mathbb{R}^d , where $\mathbf{X} = (X_1, \dots, X_d)^T$. Suppose that F_0 is a pre-specified distribution function. Given observations $\mathcal{X} = \{\mathbf{X}_1, \dots, \mathbf{X}_n\}$ independent and identically distributed (i.i.d.) from F , can we decide whether $F \neq F_0$?

Problem 2. (Two-sample multivariate problem) For $d \geq 1$, let \mathbf{X} and \mathbf{Y} be two random variables with distribution functions F and G , respectively, where $\mathbf{X} = (X_1, \dots, X_d)^T$ and $\mathbf{Y} = (Y_1, \dots, Y_d)^T$. Given the two independent data sets

$\mathcal{X} = \{\mathbf{X}_1, \dots, \mathbf{X}_n\}$ and $\mathcal{Y} = \{\mathbf{Y}_1, \dots, \mathbf{Y}_m\}$ independently and identically distributed from F and G , respectively, can we decide whether $F \neq G$?

To answer the above-mentioned questions, we propose the data-depth discrepancy (DDD) between two distributions F and G at $\mathbf{x} \in \mathbb{R}^d$ based on the data-depth as follows.

$$\text{DDD}(\mathbf{x}; F, G) = D_F(\mathbf{x}) - D_G(\mathbf{x}) \quad (7)$$

The sample version of these measures can be obtained by replacing D with its empirical data-depth values based on the specific sample sizes. Moreover, the discrepancy between the empirical and theoretical distribution is defined as $\text{DDD}(\mathbf{x}; \mathcal{X}, F_0) = D_{\mathcal{X}}(\mathbf{x}) - D_{F_0}(\mathbf{x})$. Note that, $\text{DDD}(\cdot; \cdot, \cdot)$ is valid criterion to resolve Problems 1 and 2 as long as the depth functions (here, half-space depth) characterizes the distribution. For details, see the following propositions.

Proposition 1 (Koshevoy (2002); Cuesta-Albertos and Nieto-Reyes (2008)). If F and G are two distribution functions defined on \mathbb{R}^d , both with finite support and their half-space depth coincide, then $F = G$. Moreover, if F is a discrete distribution with finite or countable support defined on \mathbb{R}^d and G is a Borel distribution on \mathbb{R}^d such that the half-space depth coincides, then $F = G$.

The characterization property of the half-space depth for discrete distributions is straightforward. For a continuous distribution function, suppose that a hyperplane Δ divides the space \mathbb{R}^d in two closed half-spaces, viz, $H_1(\Delta)$ and $H_2(\Delta)$ and $m(\Delta) = \min\{F(H_1(\Delta)), F(H_2(\Delta))\}$. Furthermore, assume B is the unit ball in \mathbb{R}^d . For $j = 1, \dots, d$, let \mathcal{S}_j^{d-1} is the relative open subspace of \mathcal{S}^{d-1} , where $\mathcal{S}_j^{d-1} = \left\{ \sum_{i=1}^d u_i \mathbf{e}_i \in \mathcal{S}^{d-1} : u_j \neq 0 \right\}$. The map $\mathbf{u} \mapsto \boldsymbol{\beta} = -\mathbf{u}/u_j$ is a diffeomorphism from one of the two connected components of \mathcal{S}_j^{d-1} into an open subset B_j of \mathbb{R}^{d-1} . Let $\boldsymbol{\beta} \in B_j$, define the hyperplane $\Delta = \Delta(\boldsymbol{\beta})$ containing a point $\mathbf{a} = (a_1, \dots, a_d)^T$ such that $\Delta(\boldsymbol{\beta}) = \{\mathbf{x} \in \mathbb{R}^d : x_j = \boldsymbol{\beta}^T(\mathbf{x} - \mathbf{a}) + a_j\}$. Thus, define two half-spaces that partitioned $\Delta(\boldsymbol{\beta})$ as $H_1(\Delta(\boldsymbol{\beta}))$ and $H_2(\Delta(\boldsymbol{\beta}))$. Now, suppose that $F_j(\boldsymbol{\beta})$ is the distribution function of $H_1(\Delta(\boldsymbol{\beta}))$ defined in \mathcal{S}_j^{d-1} , and denote the derivative of $F_j(\boldsymbol{\beta})$ with respect to $\boldsymbol{\beta}$ as $F'_j(\boldsymbol{\beta})$. If the hyperplane $\Delta(\boldsymbol{\beta})$ is a minimal hyperplane at \mathbf{a} , i.e., $m(\Delta(\boldsymbol{\beta})) = D_F(\mathbf{a})$ then F_j has an extremum in $\boldsymbol{\beta}$ and $F'_j(\boldsymbol{\beta}) = 0$. Therefore, under the condition that $F'_j(\boldsymbol{\beta}) = 0$ implies $\Delta(\boldsymbol{\beta})$ is a minimal hyperplane at \mathbf{a} , the following result holds.

Proposition 2 (Hassairi and Regaieg (2008)). Let F be a probability distribution on \mathbb{R}^d with connected support, and \mathcal{H} be the class of closed half-spaces H in \mathbb{R}^d . Assume that F is absolutely continuous with the connected support and that the corresponding probability density function is continuous with the interior of the support. Then the half-space depth characterizes the distribution.

Propositions 1 and 2 indicate that the difference of the half-space depth values can provide a valid measure of the discrepancy, which is defined as DDD in Equation (7). Now we propose a graphical method where we plot DDD as a scatter plot across a horizontal axis and measure the deviation from the horizontal axis. Needless to say, the advantage of this graphical tool-kit is that it remains unaffected by the data dimension. This graphical approach can be used for any distribution, but to produce a valid graphical tool-kit for addressing the Problems 1 and 2, we continue our discussion with half-space depth since we can exploit the characterization properties discussed in Propositions 1 and 2 of half-space depth. As a result, we can conclude that, if $\text{DDD}(\mathbf{x}; F, G) = 0$ for all \mathbf{x} , and graphically, if the majority of points are concentrated on the horizontal axis, we can conclude that the two underlying distributions are expected to be identical, where F and G belong to a certain family of distribution functions. The illustrative examples provide the different patterns of deviations from the horizontal line for both goodness-of-fit and two-sample problems.

3.1.1 Illustration of graphical tool-kit: Goodness-of-fit testing problem

For a given sample $\mathcal{X} = \{\mathbf{X}_1, \dots, \mathbf{X}_n\}$ from an unknown distribution function F , we are interested in plotting $\text{DDD}(\mathbf{x}; \mathcal{X}, F_0) = D_{\mathcal{X}}(\mathbf{x}) - D_{F_0}(\mathbf{x})$ with respect to indices of \mathbf{x} . Therefore, if two distributions are identical, then the value of $\text{DDD}(\mathbf{x}; \mathcal{X}, F_0)$ will be a straight line with respect to the observed data. Thus, this method provides some idea of goodness-of-fit. We consider four simulated data sets each consisting of 100 i.i.d. observations. Four sets of samples are generated from (1) standard bivariate normal distribution, (2) standard bivariate Cauchy distribution, (3) bivariate t-distribution with degrees of freedom (df) 3 and (4) standard bivariate Laplace distribution, respectively. For all of them, we consider the bivariate normal distribution as the specified distribution F_0 with unknown mean $\boldsymbol{\mu}$ and dispersion $\boldsymbol{\Sigma}$, that are estimated from the sample using the sample mean vector and the dispersion matrix, respectively. We standardize the sample using these estimates and see the DDD-plots based on standardized data. The data-depth discrepancy plots for the four simulated

samples are shown in Figure 1. In those plots, the dotted gray curves in the figures indicate the two-sigma limits of DDD. It is clearly evident from the graphs that the specified distribution fits the data in Figure 1a very well; moreover, the data points in this plot are clustered around the straight line and most of them are in the two-sigma limits. The other three plots 1b, 1c, 1d indicate deviations from the straight line, which immediately implies that the data are not from a normal distribution.

3.1.2 Illustration of graphical tool-kit: Two-sample testing problem

For given samples $\mathcal{X} = \{\mathbf{X}_1, \dots, \mathbf{X}_n\}$ and $\mathcal{Y} = \{\mathbf{Y}_1, \dots, \mathbf{Y}_m\}$, here we plot $\text{DDD}(\mathbf{x}; \mathcal{X}, \mathcal{Y}) = D_{\mathcal{X}}(\mathbf{x}) - D_{\mathcal{Y}}(\mathbf{x})$ for $\mathbf{x} \in \mathcal{X} \cup \mathcal{Y}$. If the two distributions are identical, then the value of $\text{DDD}(\mathbf{x}; \mathcal{X}, \mathcal{Y})$ will be in a straight line with respect to observed data. Here we consider two simulated data sets to demonstrate our proposed graphical tool-kit. In our first problem, we simulate *sample-1* consisting of 100 i.i.d. observations generated from the trivariate normal distribution having zero mean and scatter matrix $\boldsymbol{\Sigma} = (\sigma_{i,j})_{i,j=1,2,3,4}$ with $\sigma_{1,2} = 0.9$, $\sigma_{1,3} = 0.2$ and $\sigma_{2,3} = 0.5$. (*F*) and *sample-2* consisting of 50 i.i.d. observations from the standard trivariate normal distribution denoted as (*G*). In the next problem, *sample-1* consists of 100 i.i.d. observations from the standard trivariate normal distribution (*F*), and *sample-2* consists of 50 i.i.d. observations from a trivariate skew-normal distribution (*G*) (Azzalini and Valle, 1996). The p.d.f. of the trivariate skew-normal distribution is given by $f(\mathbf{x}) = 2\phi_3(\mathbf{x}; \boldsymbol{\Omega})\Phi(\boldsymbol{\alpha}^T \mathbf{x})$, where, $\boldsymbol{\alpha}^T = \frac{\boldsymbol{\lambda}^T \boldsymbol{\Psi}^{-1} \boldsymbol{\Delta}^{-1}}{\sqrt{1 + \boldsymbol{\lambda}^T \boldsymbol{\Psi}^{-1} \boldsymbol{\lambda}}}$, $\boldsymbol{\Delta} = \text{diag}(\sqrt{1 - \lambda_1^2}, \sqrt{1 - \lambda_2^2}, \sqrt{1 - \lambda_3^2})$, $\boldsymbol{\lambda} = \left(\frac{\lambda_1}{\sqrt{1 - \lambda_1^2}}, \frac{\lambda_2}{\sqrt{1 - \lambda_2^2}}, \frac{\lambda_3}{\sqrt{1 - \lambda_3^2}} \right)^T$, and $\boldsymbol{\Omega} = \boldsymbol{\Delta}(\boldsymbol{\Psi} + \boldsymbol{\lambda} \boldsymbol{\lambda}^T)\boldsymbol{\Delta}$. Here $\phi_3(\mathbf{x}; \boldsymbol{\Omega})$ denotes the probability density function of a trivariate normal distribution with standardized marginals and the correlation matrix matrix $\boldsymbol{\Omega}$, and Φ is the distribution function of the standard univariate normal distribution. In this example, we have considered $\lambda_1 = \lambda_2 = \lambda_3 = 0.9$ and $\boldsymbol{\Phi} = \mathbf{I}_3$, identity matrix of dimension 3×3 . The data-depth discrepancy plots for these two toy examples are shown in Figure 2. As before, the gray dotted curves in the figures indicate the two-sigma limits of DDD.

3.1.3 Illustration of graphical tool-kit: High-dimension data

In the last decades or so, there have been plenty of applications involved high-dimensional data, and we here illustrate the usefulness of proposed graphical tool-kit

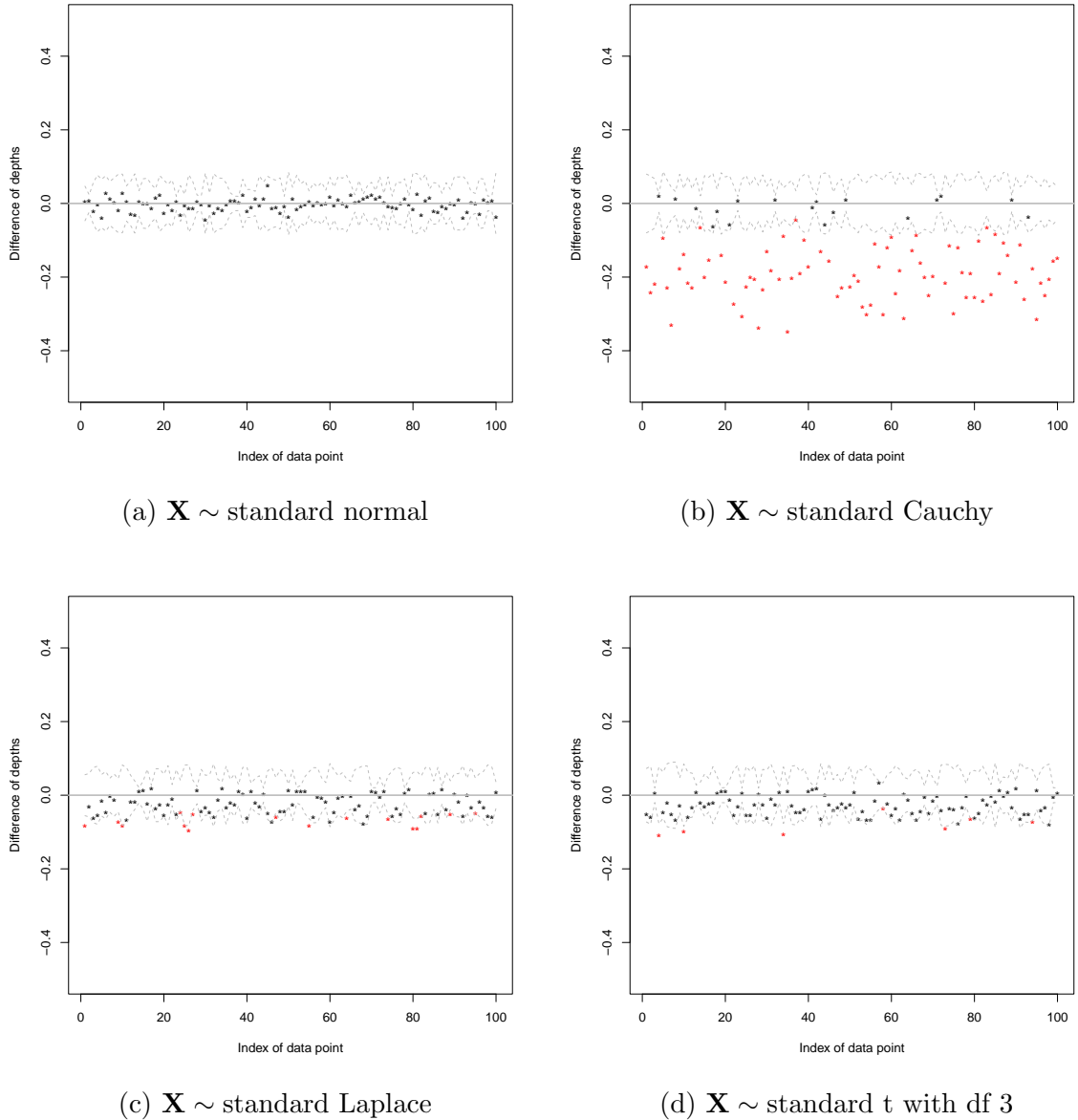
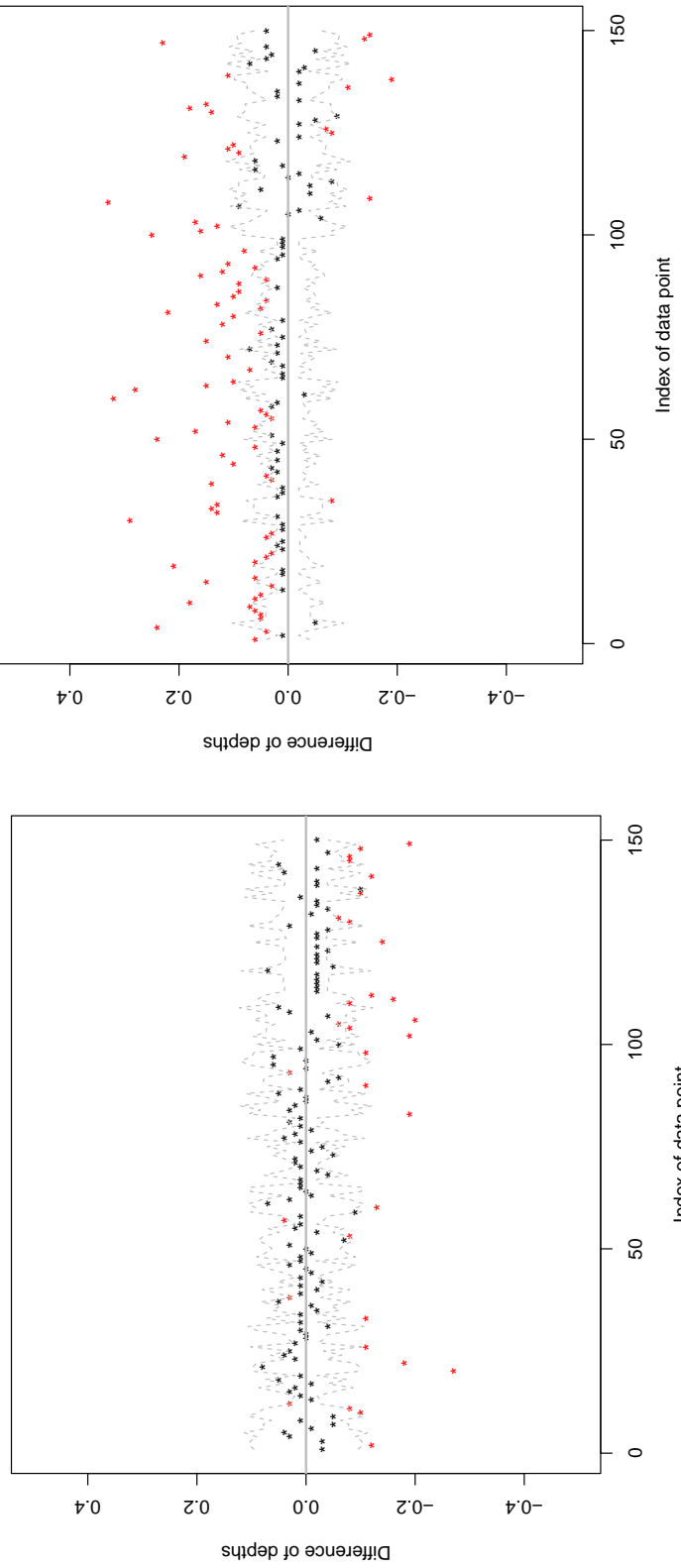


Figure 1: The data-depth discrepancy plot for the goodness-of-fit problem where the specified distribution is bivariate normal. The plots of the first and second rows are for the examples, where the distribution of the data are from bivariate standard normal, Cauchy, Laplace and t_3 distributions respectively. The dotted gray curves indicate the two-sigma limits of data-depth discrepancy. Points which are outside the two-sigma limits are color coded by red.



(a) $\mathbf{X} \sim N(0, \Sigma)$ and $\mathbf{Y} \sim N(0, \mathbf{I}_3)$
 (b) $\mathbf{X} \sim N(0, \mathbf{I}_3)$ and $\mathbf{Y} \sim f(z)$ where $f(z)$ is the p.d.f. of a skew-normal distribution

Figure 2: The data-depth discrepancy plot for the two-sample examples. The plots of the first column for an example where the sample are from trivariate normal distribution with different dispersion matrix, and those in the second column for an example, where the samples are generated from different distributions. The dotted gray curves indicate the two-sigma limits of data-depth discrepancy. Points which are outside the two-sigma limits are color coded by red.

on to meet the challenges of the modern data applications. By varying the dimensions of the data sets, $d = 10, 20, 30, 40, 50$ and 60 , we generate *sample-1* from d -variate normal distribution and *sample-2* from d -variate Cauchy distribution with sample size 100 each for a two-sample testing problem. The data-depth discrepancy plots for different dimensions are shown in Figure 3 which illustrates the fact that differences between the depth values of two samples are not clustered around the horizontal axis. This indicates that the proposed graphical tool-kit is in fact useful for high-dimensional data.

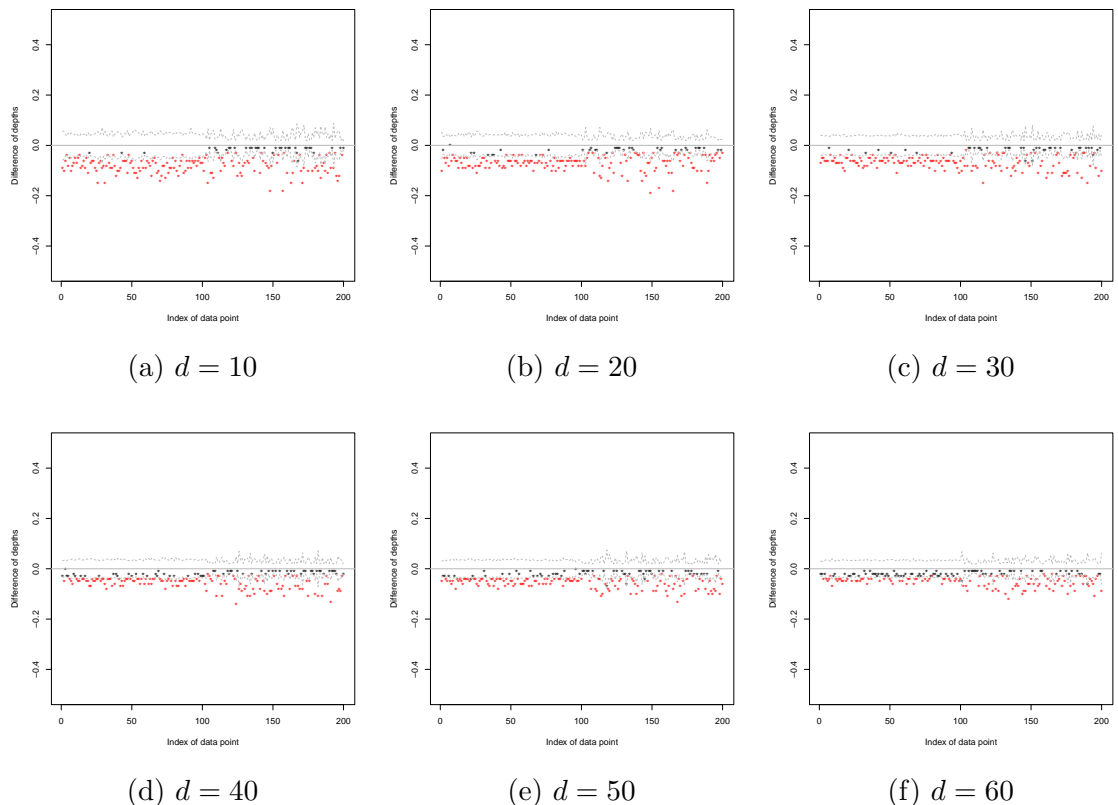


Figure 3: The data-depth discrepancy plot for the two-sample examples in high-dimensional situation for different dimensions. Here sample are from multivariate normal and Cauchy distributions. The dotted gray curves indicate the two-sigma limits of data-depth discrepancy. Points which are outside the two-sigma limits are color coded by red.

3.2 Associated tests

In Problem 1, for given sample \mathcal{X} of size n , we are interested to test $H_0 : F = F_0$ against $H_1 : F \neq F_0$, where F_0 is a pre-specified distribution function. Due to Propositions 1 and 2, for half-space depth function D , it is equivalent to test $H_0^* : D_F(\mathbf{x}) = D_{F_0}(\mathbf{x})$ for all $\mathbf{x} \in \mathbb{R}^d$ against $H_1^* : D_F(\mathbf{x}) \neq D_{F_0}(\mathbf{x})$ for some $\mathbf{x} \in \mathbb{R}^d$. The most well-known test statistics for comparing two distributions are the Kolmogorov–Smirnov (KS) test statistics and Cramér–von Mises (CvM) test statistics. These test statistics are based on the certain differences between the empirical distribution function F_n and the hypothesised distribution function F_0 . Here, we propose alternate test statistics based on these commonly known families of test statistics and DDD defined in Section 3.1 so that we can perform the goodness-of-fit test for any arbitrary dimension of the data.

1. Depth-based KS test statistic:

$$T_{\mathcal{X}, F_0}^{\text{KS}} = \sqrt{n} \sup_{\mathbf{x} \in \mathbb{R}^d} |\text{DDD}(\mathbf{x}; \mathcal{X}, F)| = \sqrt{n} \sup_{\mathbf{x} \in \mathbb{R}^d} |D_{\mathcal{X}}(\mathbf{x}) - D_{F_0}(\mathbf{x})| \quad (8)$$

2. Depth-based CvM test statistic:

$$T_{\mathcal{X}, F_0}^{\text{CvM}} = n \int \text{DDD}^2(\mathbf{x}; \mathcal{X}, F_0) dF_0(\mathbf{x}) = n \int (D_{\mathcal{X}}(\mathbf{x}) - D_{F_0}(\mathbf{x}))^2 dF_0(\mathbf{x}), \quad (9)$$

where the integral is over a closed ball in \mathbb{R}^d with the center at the origin.

For testing H_0 against H_1 , the null hypothesis will be rejected when the values of the test statistics are very large. The asymptotic behaviors of the proposed test statistics are provided in Section 4. To obtain the empirical p-value based on the proposed test statistics $T_{\mathcal{X}, F_0}$, where $T_{\mathcal{X}, F_0}$ is either $T_{\mathcal{X}, F_0}^{\text{KS}}$ or $T_{\mathcal{X}, F_0}^{\text{CvM}}$, we consider a parametric bootstrap procedure (Efron, 1982) that consists of the following steps.

Step 1.1. Generate M points uniformly from the d -dimensional unit sphere, for M sufficiently large. The set of such points is denoted as \mathcal{U} . The algorithm for generating a single sample from a d -dimensional sphere with radius r_0 is as follows.

- (a) Generate U from uniform distribution over the set $(0, r_0)$ and define $R = \sqrt{U}$.

(b) $\theta_1, \dots, \theta_{d-2} \sim \text{Uniform}(0, \pi)$, $\theta_{d-1} \sim \text{Uniform}(0, 2\pi)$ and each of θ_j s are mutually independent for $j = 1, \dots, d-1$.

(c) A d -dimensional observation from the sphere is $\mathbf{u} = (u_1, \dots, u_d)^T$ where,

$$\begin{aligned} u_1 &= R \cos \theta_1 \\ u_2 &= R \sin \theta_1 \cos \theta_2 \\ &\vdots \\ u_{d-1} &= R \sin \theta_1 \sin \theta_2 \dots \sin \theta_{d-2} \cos \theta_{d-1} \\ u_d &= R \sin \theta_1 \sin \theta_2 \dots \sin \theta_{d-2} \sin \theta_{d-1}. \end{aligned}$$

Step 1.2. Calculate half-space depth with respect to samples \mathcal{X} and F_0 , respectively, and therefore, calculate $\text{DDD}(\mathbf{x}; \mathcal{X}, F_0)$ for all $\mathbf{x} \in \mathcal{U}$. Construct an approximate test statistic $\tilde{T}_{\mathcal{X}, F_0}$ which is either $\tilde{T}_{\mathcal{X}, F_0}^{\text{KS}} = \sqrt{n} \max_{\mathbf{x} \in \mathcal{U}} |\text{DDD}(\mathbf{x}; \mathcal{X}, F_0)|$ or $\tilde{T}_{\mathcal{X}, F_0}^{\text{CvM}} = n \times \frac{1}{M} \sum_{j=1}^M \text{DDD}^2(\mathbf{x}_j; \mathcal{X}, F_0)$ based on the choice of $T_{\mathcal{X}, F_0}$.

Step 1.3. Let θ be the unspecified parameter of the distribution function F_0 (denoted as $F_0(\cdot; \theta)$) and $\hat{\theta}_n$ be an estimate of θ which could be the maximum likelihood estimate.

Step 1.4. Draw a random sample $\mathcal{X}^* = \{\mathbf{X}_1^*, \dots, \mathbf{X}_n^*\}$ from fitted distribution $F_0(\cdot; \hat{\theta}_n)$.

Step 1.5. Compute the half-space depth with respect to \mathcal{X}^* and, therefore, compute $\text{DDD}(\mathbf{x}; \mathcal{X}^*, F_0(\cdot; \hat{\theta}_n)) = D_{\mathcal{X}^*}(\mathbf{x}) - D_{F_0(\cdot; \hat{\theta}_n)}(\mathbf{x})$ for $\mathbf{x} \in \mathcal{U}$. Thus, calculate the test statistic $\tilde{T}_{\mathcal{X}^*, F_0(\cdot; \hat{\theta}_n)}$ based on $\text{DDD}(\mathbf{x}; \mathcal{X}^*, F_0(\cdot; \hat{\theta}_n))$.

Step 1.6. Repeat Steps 1.4 and 1.5 for B times, where B is sufficiently large. Thus, the empirical distribution of $\{\tilde{T}_{\mathcal{X}^*, F_0(\cdot; \hat{\theta}_n)}^{(b)} : b = 1, \dots, B\}$ can be used to approximate the null distribution of $T_{\mathcal{X}, F_0}$.

Step 1.7. The empirical p-value is computed using the following formula.

$$\hat{\mathbb{P}}_{H_0} \left\{ T_{\mathcal{X}, F_0} > \tilde{T}_{\mathcal{X}, F_0} \right\} = \frac{1}{B} \sum_{b=1}^B \mathbf{1} \left\{ \tilde{T}_{\mathcal{X}^*, F_0(\cdot; \hat{\theta}_n)}^{(b)} > \tilde{T}_{\mathcal{X}, F_0} \right\} \quad (10)$$

Next, we consider the two-sample d -dimensional problem for two independent samples

$\mathcal{X} = \{\mathbf{X}_1, \dots, \mathbf{X}_n\}$ and $\mathcal{Y} = \{\mathbf{Y}_1, \dots, \mathbf{Y}_m\}$ where \mathbf{X}_i 's are independently distributed with distribution function F and \mathbf{Y}_i 's are independently distributed with distribution function G . In Problem 2, we want to test $H_0 : F = G$ against $H_1 : F \neq G$, which is equivalent to test $H_0^* : D_F(\mathbf{x}) = D_G(\mathbf{x})$ for all $\mathbf{x} \in \mathbb{R}^d$ against $H_1^* : D_F(\mathbf{x}) \neq D_G(\mathbf{x})$ for some $\mathbf{x} \in \mathbb{R}^d$, where D is the half-space depth. Similar to goodness-of-fit test problem, the above testing procedure is meaningful due to the characterization property of half-space depth. We construct the KS and CvM type test statistics based on $\text{DDD}(\mathbf{x}; \mathcal{X}, \mathcal{Y})$ and obtain the following test statistics.

1. Depth-based KS test statistic:

$$T_{\mathcal{X}, \mathcal{Y}}^{\text{KS}} = \sqrt{n+m} \sup_{\mathbf{x} \in \mathbb{R}^d} |\text{DDD}(\mathbf{x}; \mathcal{X}, \mathcal{Y})| = \sqrt{n+m} \sup_{\mathbf{x} \in \mathbb{R}^d} |D_{\mathcal{X}}(\mathbf{x}) - D_{\mathcal{Y}}(\mathbf{x})| \quad (11)$$

2. Depth-based CvM test statistic:

$$T_{\mathcal{X}, \mathcal{Y}}^{\text{CvM}} = (n+m) \int \text{DDD}^2(\mathbf{x}; \mathcal{X}, \mathcal{Y}) dH_{n,m}(\mathbf{x}) = (n+m) \int (D_{\mathcal{X}}(\mathbf{x}) - D_{\mathcal{Y}}(\mathbf{x}))^2 dH_{n,m}(\mathbf{x}), \quad (12)$$

where the integral is over a closed ball in \mathbb{R}^d with the center at origin, and $H_{n,m}(\cdot)$ is the empirical distribution function based on the combine sample $\mathcal{X} \cup \mathcal{Y}$.

Here also, for large value of the test statistics, we reject the null hypothesis. The asymptotic results for the proposed test statistics are studied in Section 4. The following algorithm provides an empirical p-value (Tibshirani and Efron, 1993) for Problem 2 based on any of the proposed test statistics $T_{\mathcal{X}, \mathcal{Y}}$ where $T_{\mathcal{X}, \mathcal{Y}}$ is either $T_{\mathcal{X}, \mathcal{Y}}^{\text{KS}}$ or $T_{\mathcal{X}, \mathcal{Y}}^{\text{CvM}}$.

Step 2.1. Generate M points uniformly from the d -dimensional unit sphere, for sufficiently large M . The set of such points is denoted as \mathcal{U} .

Step 2.2. Calculate half-space depth with respect to samples \mathcal{X} and \mathcal{Y} respectively, and therefore compute $\text{DDD}(\mathbf{x}; \mathcal{X}, \mathcal{Y})$ for all $\mathbf{x} \in \mathcal{U}$. Construct an approximate test statistic $\tilde{T}_{\mathcal{X}, \mathcal{Y}}$ which is either $\tilde{T}_{\mathcal{X}, \mathcal{Y}}^{\text{KS}} = \sqrt{n+m} \max_{\mathbf{x} \in \mathcal{U}} |\text{DDD}(\mathbf{x}; \mathcal{X}, \mathcal{Y})|$ or $\tilde{T}_{\mathcal{X}, \mathcal{Y}}^{\text{CvM}} = (n+m) \times \frac{1}{M} \sum_{j=1}^M \text{DDD}^2(\mathbf{x}_j; \mathcal{X}, \mathcal{Y})$.

Step 2.3. Combine the samples \mathcal{X} and \mathcal{Y} , and the pooled sample is denoted as $\mathcal{Z} = \{\mathbf{X}_1, \dots, \mathbf{X}_n\} \cup \{\mathbf{Y}_1, \dots, \mathbf{Y}_m\}$.

Step 2.4. For the b -th bootstrap replicate, take a sample of size $(n + m)$ from \mathcal{Z} with replacement and treat the first n as the \mathcal{X}_b^* sample and the last m are \mathcal{Y}_b^* for $b = 1, \dots, B$, where B is sufficiently large.

Step 2.5. Compute half-space depths based on the samples \mathcal{X}_b^* and \mathcal{Y}_b^* separately for each of the replicates. Therefore, compute the approximate test statistic $\tilde{T}_{\mathcal{X}^*, \mathcal{Y}^*}^{(b)}$ as described in Step 2.2 by replacing \mathcal{X} with \mathcal{X}_b^* and \mathcal{Y} with \mathcal{Y}_b^* . Thus, the empirical distribution of $\tilde{T}_{\mathcal{X}^*, \mathcal{Y}^*}^{(b)}$'s can be used to approximate the null distribution of $T_{\mathcal{X}, \mathcal{Y}}$.

Step 2.6. The empirical p-value is computed using the following formula.

$$\hat{\mathbb{P}}_{H_0} \left\{ T_{\mathcal{X}, \mathcal{Y}} > \tilde{T}_{\mathcal{X}, \mathcal{Y}} \right\} = \frac{1}{B} \sum_{b=1}^B \mathbf{1} \left\{ \tilde{T}_{\mathcal{X}^*, \mathcal{Y}^*}^{(b)} > \tilde{T}_{\mathcal{X}, \mathcal{Y}} \right\} \quad (13)$$

Remark 1. Using the Algorithms described above, it is observed that the computation of the p-values is simple and efficient enough even when the dimension of the data is fairly large.

4 Main results

In the earlier section, we studied the algorithms to compute the p-value of the tests. However, one needs to know the distribution of the test statistics to estimate the size and power of the tests. Observe that the derivation of the exact distribution of the test statistics is intractable because of its complex expression, and to overcome this issue, this section investigates the asymptotic consistency and the asymptotic power under contiguous alternatives of the proposed test using the asymptotic distribution of the test statistics.

4.1 Large sample properties

To investigate the asymptotic properties of the proposed graphical tool-kit and tests, one first needs to assume a few technical conditions.

Suppose that $\mathbf{X}_1, \dots, \mathbf{X}_n$ are the multivariate observations from an unknown distribution F , and the corresponding empirical distribution function is denoted by

\widehat{F}_n . We define $\mathcal{L}_n(\mathbf{x}) = \sqrt{n}(D_{\mathcal{X}}(\mathbf{x}) - D_F(\mathbf{x}))$ for $\mathbf{x} \in \mathbb{R}^d$. Therefore, $\{\mathcal{L}_n : \mathbf{x} \in \mathbb{R}^d\}$ is a stochastic process with bounded sample path which is a map into $l^\infty(\mathbb{R}^d)$, a space of bounded real valued function on \mathbb{R}^d equipped with the uniform norm, viz., $\|a\|_\infty = \sup_{\mathbf{t} \in \mathbb{R}^d} |a(\mathbf{t})|$. Moreover, define $\mathcal{V}_n = \sqrt{n}(\widehat{F}_n - F)$, and that can be viewed as a map into space $l^\infty(\mathcal{H})$, where \mathcal{H} is the class of closed half-spaces H in \mathbb{R}^d . The technical assumptions:

- (C1) Let ∂H be the topological boundary of H . Then the distribution function F satisfies $F(\partial H) = 0$ for all $H \in \mathcal{H}$.
- (C2) Let \mathcal{F} be a point-wise bounded, totally bounded and permissible subset of $L_2(F)$ on \mathcal{H} , where $L_2(F)$ is the set of all square-integrable functions with respect to F . For each $\eta > 0$ and $\epsilon > 0$, there exists a $\delta > 0$ such that, $\limsup \mathbb{P} \{ \sup_{\mathcal{D}(\delta)} |\mathcal{V}_n(f - g)| > \eta \} < \epsilon$, where $\mathcal{D}(\delta) = \{(f, g) : f, g \in \mathcal{F}, \rho_F(f - g) < \delta\}$ for the semi-norm ρ_F on \mathcal{H} .
- (C3) At any point with positive depth, the collection of all minimal directions passing through that point has a finite number of elements or equals with $\mathcal{S}^{d-1} = \{\mathbf{u} : \|\mathbf{u}\| = 1\}$.
- (C4) A minimal closed half-space at \mathbf{x} , viz. $H[\mathbf{x}]$ is uniquely defined if $D_F(\mathbf{x}) > 0$.
- (C5) The distribution functions are either with finite support or absolutely continuous with continuous probability density function.

Remark 2. (C1) is the smoothness condition of the underlying distribution function. This is useful to obtain the stronger properties of the Tukey's half-space depth in different applications. For example, it is easy to see that if F is absolutely continuous, the condition (C1) is satisfied (Massé, 2004). Moreover, if F satisfies (C1), $D_F(\mathbf{x})$ can be expressed as the probability of some closed half-space whose boundary goes through \mathbf{x} . In addition to that, for the closed half-space $H[\mathbf{x}, \mathbf{u}] = \{\mathbf{y} \in \mathbb{R}^d : \mathbf{u}^T \mathbf{x} \geq \mathbf{u}^T \mathbf{y}\}$, the function $(\mathbf{x}, \mathbf{u}) \mapsto F(H[\mathbf{x}, \mathbf{u}])$ is continuous on $\mathbb{R}^d \times \mathcal{S}^{d-1}$ and $\mathbf{x} \mapsto D_F(\mathbf{x})$ is continuous. Condition (C2) are useful for empirical central limit theorems (see Pollard (1984)). If $D(\mathbf{x}) = F(H[\mathbf{x}, \mathbf{u}])$, $H[\mathbf{x}, \mathbf{u}]$ is a minimal half-space at \mathbf{x} and \mathbf{u} is a minimal direction at the same point. (C3) satisfies the condition related to the multiplicity of the minimal direction at \mathbf{x} . The conditions (C1) and (C3) are referred as the “local regularity conditions” in the literature. The details about the condition (C5) is discussed in Propositions 1 and 2.

Proposition 3 states the weak convergence of \mathcal{V}_n .

Proposition 3. (Theorem 21 in section VII.5 of Pollard (1984)) Under condition (C2), $\mathcal{V}_n = \sqrt{n}(\widehat{F}_n - F)$ converges weakly to \mathcal{V}_F where \mathcal{V}_F is tight and F -Brownian bridge with mean zero and covariance function $\Sigma_F = F(H_1 \cap H_2) - F(H_1)F(H_2)$ for $H_1, H_2 \in \mathcal{H}$. Moreover, \mathcal{V}_F can be chosen such that each sample path is continuous with respect to ρ .

Let us define $\mathcal{J}(\mathcal{V}_F)(\mathbf{x}) = \inf_{\mathbf{v} \in V(\mathbf{x})} \mathcal{V}_F H[\mathbf{x}, \mathbf{v}]$ for $\mathbf{x} \in \mathbb{R}^d$, where $V(\mathbf{x})$ is the set of all minimal directions passing thought that point. Proposition 4 states the asymptotic distribution of the Tukey's half-space depth.

Proposition 4. (Massé, 2004) Under the conditions (C1)-(C4), for A is a closed subset of \mathcal{S}_F , in $l^\infty(A)$, $\{\mathcal{L}_n\}$ converges weakly to $\mathcal{J}(\mathcal{V}_F)$, which is tight measurable map into $l^\infty(A)$. Moreover, $\mathcal{J}(\mathcal{V}_F)$ is a random element associated with a centered Gaussian process with covariance function $\text{cov}\{\mathcal{J}(\mathcal{V}_F)(\mathbf{x}_1), \mathcal{J}(\mathcal{V}_F)(\mathbf{x}_2)\} = F(H[\mathbf{x}_1] \cap H[\mathbf{x}_2]) - F(H[\mathbf{x}_1])F(H[\mathbf{x}_2])$ for $\mathbf{x}_1, \mathbf{x}_2 \in A$.

We now state the results, which justifies the usefulness of the proposed graphical tool-kits for sufficiently large sample sizes. See Theorems 1 and 2:

Theorem 1. For every $\epsilon > 0$, define $\mathcal{C}_\epsilon(F, F_0) = \{(\mathbf{x}, D_F(\mathbf{x}) - D_{F_0}(\mathbf{x})) : \mathbf{x} \in \mathbb{R}^d, |D_F(\mathbf{x}) - D_{F_0}(\mathbf{x})| < \epsilon\}$ and for a given sample $\mathcal{X} = \{\mathbf{X}_1, \dots, \mathbf{X}_n\}$, $\widehat{\mathcal{C}}(\mathcal{X}, F_0) = \{(\mathbf{x}, D_{\mathcal{X}}(\mathbf{x}) - D_{F_0}(\mathbf{x})) : \mathbf{x} \in \mathcal{X}\}$. Then, under the conditions (C1)-(C5),

$$\lim_{n \rightarrow \infty} \mathbb{P} \left\{ \widehat{\mathcal{C}}(\mathcal{X}, F_0) \subset \mathcal{C}_\epsilon(F, F_0) \right\} = 1. \quad (14)$$

Theorem 2. For every $\epsilon > 0$, define $\mathcal{C}_\epsilon(F, G) = \{(\mathbf{x}, D_F(\mathbf{x}) - D_G(\mathbf{x})) : \mathbf{x} \in \mathbb{R}^d, |D_F(\mathbf{x}) - D_G(\mathbf{x})| < \epsilon\}$ and for given independent samples $\mathcal{X} = \{\mathbf{X}_1, \dots, \mathbf{X}_n\}$ and $\mathcal{Y} = \{\mathbf{Y}_1, \dots, \mathbf{Y}_m\}$, $\widehat{\mathcal{C}}(\mathcal{X}, \mathcal{Y}) = \{(\mathbf{x}, D_{\mathcal{X}}(\mathbf{x}) - D_{\mathcal{Y}}(\mathbf{x})) : \mathbf{x} \in \mathcal{X} \cup \mathcal{Y}\}$. Then, under the conditions (C1)-(C5), for positive finite number $\lambda = \lim_{\min(n, m) \rightarrow \infty} n/(n + m)$,

$$\lim_{\min(n, m) \rightarrow \infty} \mathbb{P} \left\{ \widehat{\mathcal{C}}(\mathcal{X}, \mathcal{Y}) \subset \mathcal{C}_\epsilon(F, G) \right\} = 1. \quad (15)$$

Remark 3. Theorems 1 and 2 show that for large sample size the points in the sets lie around the horizontal axis if and only if the null hypothesis is expected to be true for both the goodness-of-fit and two-sample testing problem under some mild conditions.

Next, Theorems 3 and 4 assert the point-wise asymptotic properties of the goodness-of-fit tests based on $T_{\mathcal{X}, F_0}^{\text{KS}}$ and $T_{\mathcal{X}, F_0}^{\text{CvM}}$.

Theorem 3. Under the conditions (C1)-(C5), the test based on test statistic $T_{\mathcal{X}, F_0}^{\text{KS}}$ for testing $H_0 : F = F_0$ against $H_1 : F \neq F_0$ is point-wise consistent in power, i.e., $\mathbb{P}_F\{T_{\mathcal{X}, F_0}^{\text{KS}} > s_{1-\alpha}^{(1)}\} \rightarrow 1$ as $n \rightarrow \infty$ under H_1 , where $s_{1-\alpha}^{(1)}$ is such that $\lim_{n \rightarrow \infty} \mathbb{P}_{H_0}\{T_{\mathcal{X}, F_0}^{\text{KS}} > s_{1-\alpha}^{(1)}\} = \alpha$.

Theorem 4. Under the conditions (C1)-(C5), the test based on test statistic $T_{\mathcal{X}, F_0}^{\text{CvM}}$ for testing $H_0 : F = F_0$ against $H_1 : F \neq F_0$ is point-wise consistent in power, i.e., $\mathbb{P}\{T_{\mathcal{X}, F_0}^{\text{CvM}} > s_{1-\alpha}^{(2)}\} \rightarrow 1$ as $n \rightarrow \infty$, where $s_{1-\alpha}^{(2)}$ is such that $\lim_{n \rightarrow \infty} \mathbb{P}_{H_0}\{T_{\mathcal{X}, F_0}^{\text{CvM}} > s_{1-\alpha}^{(2)}\} = \alpha$.

Now, Theorems 5 and 6 assert the asymptotically uniform power properties of the goodness-of-fit test based on $T_{\mathcal{X}, F_0}^{\text{KS}}$ and $T_{\mathcal{X}, F_0}^{\text{CvM}}$.

Theorem 5. Suppose that $\mathcal{X} = \{\mathbf{X}_1, \dots, \mathbf{X}_n\}$ is a collection of i.i.d. random variables with distribution function F . For testing $F = F_0$ against $H_1 : F \neq F_0$, under the conditions (C1)-(C5), the power of the test based on $T_{\mathcal{X}, F_0}^{\text{KS}}$ tends to 1 uniformly over all alternatives F satisfying $\sqrt{n}d_K(D_F, D_{F_0}) \geq \Delta_n$, if $\Delta_n \rightarrow \infty$ as $n \rightarrow \infty$.

Theorem 6. Suppose that $\mathcal{X} = \{\mathbf{X}_1, \dots, \mathbf{X}_n\}$ is a collection of i.i.d. random variables with distribution function F . For testing $H_0 : F = F_0$ against $H_1 : F \neq F_0$, under the conditions (C1)-(C5), the power of test based on $T_{\mathcal{X}, F_0}^{\text{CvM}}$ tends to 1 uniformly over all alternatives F_n satisfying $\sqrt{n}d_K(D_{F_n}, D_{F_0}) \geq \Delta_n$ if $\Delta_n \rightarrow \infty$ as $n \rightarrow \infty$.

We now describe the results related to point-wise and uniform consistency of the proposed two-sample testing procedure.

Theorem 7. Let us denote $T_{\mathcal{X}, \mathcal{Y}}^{(1)} := T_{\mathcal{X}, \mathcal{Y}}^{\text{KS}}$ and $T_{\mathcal{X}, \mathcal{Y}}^{(2)} := T_{\mathcal{X}, \mathcal{Y}}^{\text{CvM}}$, and n and m are such that $\lim_{\min(n, m) \rightarrow \infty} \frac{n}{n+m} = \lambda \in (0, 1)$. For $i = 1$ and 2 , let $t_{1-\alpha}^{(i)}$ be such that $\lim_{\min(n, m) \rightarrow \infty} \mathbb{P}_{H_0}\{T_{\mathcal{X}, \mathcal{Y}}^{(i)} > t_{1-\alpha}^{(i)}\} = \alpha$. Further, suppose that $H(\mathbf{x}) = \lambda F(\mathbf{x}) + (1 - \lambda)G(\mathbf{x})$ and $\int(D_F(\mathbf{x}) - D_G(\mathbf{x}))dH(\mathbf{x}) < \infty$. Then, under the conditions (C1)-(C5), $\mathbb{P}_{H_1}\{T_{\mathcal{X}, \mathcal{Y}}^{(i)} > t_{1-\alpha}^{(i)}\} \rightarrow 1$, as $\min(n, m) \rightarrow \infty$. Moreover, for $i = 1$ and 2 , the power of the test based on $T_{\mathcal{X}, \mathcal{Y}}^{(i)}$ tends to one, uniformly over all alternatives satisfying $\sqrt{n+m}d_k(D_{F_n}, D_{G_m}) \geq \Delta_{m,n}$ if $\Delta_{m,n} \rightarrow \infty$ as $\min(m, n) \rightarrow \infty$.

4.2 Asymptotic local power study

In Section 4.1, we have established that data-depth based KS and CvM tests are all asymptotically consistent, and therefore, a natural question is how is the asymptotic power of the tests under local/contiguous alternatives (see Sidak et al. (1999)). Let \mathbb{P}_n and \mathbb{Q}_n be the sequences of the probability measures defined on sequence of probability spaces $(\Omega_n, \mathcal{A}_n)$. Then, \mathbb{Q}_n is said to be contiguous with respect to \mathbb{P}_n when $\mathbb{P}_n\{A_n\} \rightarrow 0$ implies that $\mathbb{Q}_n\{A_n\} \rightarrow 0$ for every sequence of measurable sets A_n . It is important to note that the sequence of set A_n changes with n along with the σ -field \mathcal{A}_n , and hence, it does not directly follow from the definition of contiguity that any distribution function \mathbb{Q}_n is contiguous with respect to \mathbb{P}_n . In order to characterize the contiguity in terms of the asymptotic behavior of the likelihood ratio between \mathbb{P}_n and \mathbb{Q}_n , Le Cam proposed some results which are popularly known as “Le Cam’s Lemma”. A consequence of Le Cam’s first lemma is that the sequence \mathbb{Q}_n will be contiguous with respect to the sequence \mathbb{P}_n if $\log(\mathbb{Q}_n/\mathbb{P}_n)$ is an asymptotically normal random variable with mean $-\sigma^2/2$ and variance σ^2 , where σ is a positive constant. Moreover, the consequence of Le Cam’s third lemma is that for $\mathbf{X}_n \in \mathbb{R}^d$, the joint distribution of \mathbf{X}_n and $\log(\mathbb{Q}_n/\mathbb{P}_n)$ is distributed as multivariate normal with mean vector $(\boldsymbol{\mu}, -\sigma^2/2)^T$ and covariance $\begin{pmatrix} \boldsymbol{\Sigma} & \boldsymbol{\tau} \\ \boldsymbol{\tau}^T & \sigma^2 \end{pmatrix}$ under \mathbb{P}_n , then under the alternative distribution \mathbb{Q}_n , the asymptotic distribution of \mathbf{X} is also a normal with mean $\boldsymbol{\mu} + \boldsymbol{\tau}$ and covariance $\boldsymbol{\Sigma}$.

In order to test $H_0 : F = F_0$, we consider the sequence of alternatives

$$H_n : F_n = \left(1 - \frac{\gamma}{\sqrt{n}}\right) F_0 + \frac{\gamma}{\sqrt{n}} H \quad (16)$$

for a fixed $\gamma > 0$ and $n = 1, 2, \dots$. In terms of depth function, this testing of hypothesis problem can equivalently be written as $H_0^* : D_F = D_{F_0}$, and the sequence of alternatives $H_n^* : D_{F_n} = (1 - \frac{\gamma}{\sqrt{n}}) D_{F_0} + \frac{\gamma}{\sqrt{n}} D_H$. It follows from the Propositions 1 and 2 that the aforesaid hypothesis statement is valid for half-space depth function. Theorems 8 and 9 state the asymptotic power properties of the proposed test.

Theorem 8. Assume that F_0 and H (see (16)) have continuous and positive densities f_0 and h , respectively on \mathbb{R}^d ($d \geq 2$) such that $\mathbb{E}_{H_0} \left\{ \frac{h(\mathbf{x})}{f_0(\mathbf{x})} - 1 \right\}^4 < \infty$, and suppose that the optimal half-space depth associated to \mathbf{x} is unique. In addition, conditions (C1)-(C5) hold. Then the sequence of alternatives is a contiguous sequence. Further, assume that $\mathcal{G}_1(\mathbf{x})$ is a random element associated with a Gaussian process with

mean function zero and covariance kernel $F_0(H[\mathbf{x}_1] \cap H[\mathbf{x}_2]) - F_0(H[\mathbf{x}_1])F_0(H[\mathbf{x}_2])$, and $\mathcal{G}'_1(\mathbf{x})$ is a random element associated with a Gaussian process with mean function $-\gamma \mathbb{E}_{\mathbf{x} \sim h} \{D_{F_0}(\mathbf{x})\}$ and covariance kernel $F_0(H[\mathbf{x}_1] \cap H[\mathbf{x}_2]) - F_0(H[\mathbf{x}_1])F_0(H[\mathbf{x}_2])$. Under the alternatives described in (16), the asymptotic power of the test based on $T_{\mathcal{X}, F_0}^{\text{KS}}$ is $\mathbb{P}_\gamma \left\{ \sup_{\mathbf{x}} |\mathcal{G}'_1(\mathbf{x})| > s_{1-\alpha}^{(1)} \right\}$, where $s_{1-\alpha}^{(1)}$ is such that $\mathbb{P}_{\gamma=0} \left\{ \sup_{\mathbf{x}} |\mathcal{G}_1(\mathbf{x})| > s_{1-\alpha}^{(1)} \right\} = \alpha$. Moreover, under the alternative hypothesis described in (16), the asymptotic power of the test based on $T_{\mathcal{X}, F_0}^{\text{CvM}}$ is $\mathbb{P}_\gamma \left\{ \int |\mathcal{G}'_1(\mathbf{x})|^2 dF_0(\mathbf{x}) > s_{1-\alpha}^{(2)} \right\}$, where $s_{1-\alpha}^{(2)}$ is such that $\mathbb{P}_{\gamma=0} \left\{ \int |\mathcal{G}_1(\mathbf{x})|^2 dF_0(\mathbf{x}) > s_{1-\alpha}^{(2)} \right\} = \alpha$.

Now consider the scenario of a two-sample problem. The null hypothesis is given by $H_0 : F = G$ against the sequences of alternatives

$$H_{n,m} : G = \left(1 - \frac{\gamma}{\sqrt{n+m}}\right) F + \frac{\gamma}{\sqrt{n+m}} H \quad (17)$$

for a fixed $\gamma > 0$ and $n, m = 1, 2, \dots$, which is equivalent to test $H_0^* : D_F = D_G$ against the sequence of alternatives $H_{n,m}^* : D_G = \left(1 - \frac{\gamma}{\sqrt{n+m}}\right) D_F + \frac{\gamma}{\sqrt{n+m}} D_H$.

Theorem 9. Assume F and H (see (17)) have continuous and positive densities f and h , respectively on \mathbb{R}^d ($d \geq 2$) such that $\mathbb{E}_F \left\{ \frac{h(\mathbf{x})}{f(\mathbf{x})} - 1 \right\}^4 < \infty$. Suppose that the optimal half-space depth associated to \mathbf{x} is unique and $\lim_{\min(n,m) \rightarrow \infty} \frac{n}{m+n} = \lambda \in (0, 1)$, and in addition, conditions (C1)-(C5) hold. Then the sequence of alternatives is a contiguous sequence. Furthermore, assume that $\mathcal{G}_2(\mathbf{x})$ is a random element associated with a Gaussian process with mean function zero and covariance kernel $\{F(H[\mathbf{x}_1] \cap H[\mathbf{x}_2]) - F(H[\mathbf{x}_1])F(H[\mathbf{x}_2])\} / \lambda(1 - \lambda)$ and $\mathcal{G}'_2(\mathbf{x})$ is a random element associated with a Gaussian process with mean function $\gamma \sqrt{\lambda/(1 - \lambda)} \mathbb{E}_{\mathbf{u} \sim h} \{D_F(\mathbf{x})\}$ and covariance kernel $\{F(H[\mathbf{x}_1] \cap H[\mathbf{x}_2]) - F(H[\mathbf{x}_1])F(H[\mathbf{x}_2])\} / \lambda(1 - \lambda)$. Under the alternatives described in (17), the asymptotic power of the test based on KS is $\mathbb{P}_\gamma \{\sup_{\mathbf{x}} |\mathcal{G}'_2(\mathbf{x})| > t_{1-\alpha}^{(1)}\}$ where $t_{1-\alpha}^{(1)}$ is such that $\mathbb{P}_{\gamma=0} \{\sup_{\mathbf{x}} |\mathcal{G}_2(\mathbf{x})| > t_{1-\alpha}^{(1)}\} = \alpha$. Moreover, under the alternative hypothesis described in (17), the asymptotic power of the test based on CvM is $\mathbb{P}_\gamma \left\{ \int |\mathcal{G}'_2(\mathbf{x})|^2 d\mathbf{x} > t_{1-\alpha}^{(2)} \right\}$ where $\mathbb{P}_{\gamma=0} \left\{ \int |\mathcal{G}'_2(\mathbf{x})|^2 d\mathbf{x} > t_{1-\alpha}^{(2)} \right\} = \alpha$.

The results in Theorems 8 and 9 provide us the asymptotic power of the proposed tests under the local alternatives described in (16) and (17), respectively. Using those results, we compute the asymptotic powers of the proposed tests for various choices of

γ . In this study, we consider that F_0 is the standard bivariate normal distribution, and H is the standard bivariate Laplace distribution. Figure 4 illustrate the summarised results, and it is clearly indicated by those diagram that our proposed tests perform well for this example. For the sake of concise presentation, we are not reporting here the results for other choices of F_0 and H , and some other choices of dimension. Nevertheless, our preliminary investigation suggests that the tests perform well for alternative choices also.

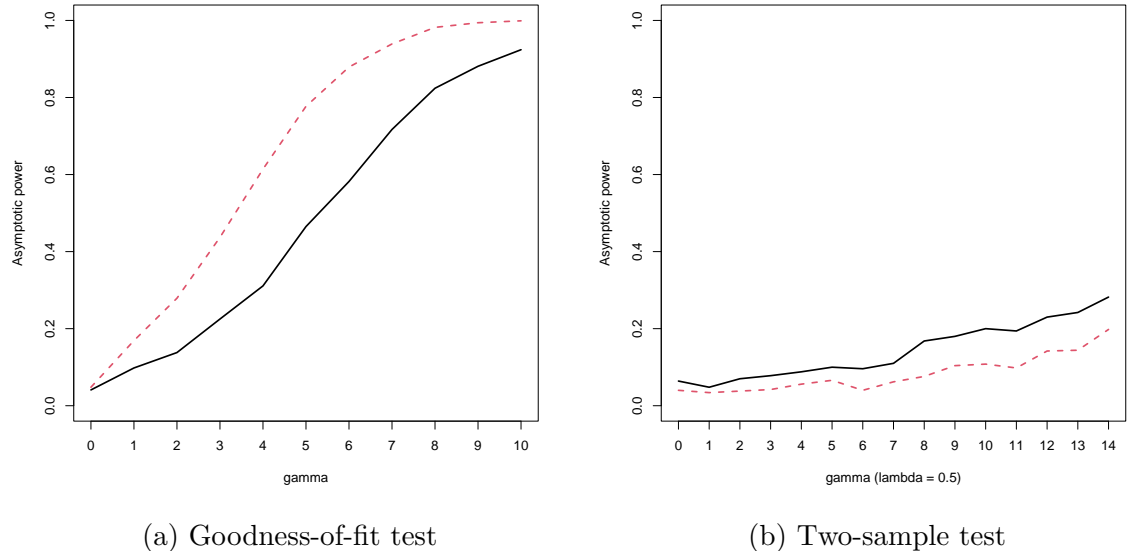


Figure 4: The asymptotic power for (a) goodness-of-fit test and (b) two-sample test with $\lambda = 0.5$ under contiguous alternative described in (16) and (17), respectively, where F_0 is standard bivariate normal distribution and H is the standard Laplace distribution. The black solid line indicates the results based on proposed depth-based KS test statistics and the red dotted line indicates the results based on proposed depth-based CvM test statistics.

5 Simulation studies

In this section, we demonstrate the finite sample performance by reporting the size and power of the proposed tests obtained from multiple studies compared to other existing methods. In order to implement the proposed tests, we prepared R codes which are available at <https://github.com/pratimguhaniyogi>. Precisely speaking,

we use `mvtnorm` and `LaplacesDemon` to generate the data from multivariate normal, t and Laplace distributions, respectively. Next, in order to compute the half-space depth, the package, viz., `ddalpha` is used. For other details, the users are referred to the aforementioned web-link. Next, in order to implement the other tests, `mvnTest` is used to run goodness-of-fit tests. All the simulation results in the following examples are based on 500 replications, and the critical value of the test is estimated by 500 bootstrap samples in each of the simulation runs. We also study the simulation results for cases with different dimensions, choosing $d \in \{2, 6, 10\}$. Furthermore, we denote $\mu \in \mathbb{R}^d$ as a location parameter and Σ is a $d \times d$ positive definite matrix as a scale parameter in those examples.

In the goodness-of-fit problem (see Problem 1), we assume that F_0 is a standard d -dimensional normal distribution. The choices of unknown distributions described in Problem 1 are listed below.

Model A.1. Standard d -variate normal distribution $N_d(\mathbf{0}_d, \mathbf{I}_d)$, where $\mathbf{0}_d = (0, \dots, 0)^T$ is the d -dimensional null vector, and \mathbf{I}_d refers to the $d \times d$ identity matrix.

Model A.2. Mixture of the d -variate normal distribution with mixing probability 0.8, where the samples are taken from $0.8N_d(\mathbf{0}_d, \mathbf{I}_d) + 0.2N_d(5 \times \mathbf{1}_d, \mathbf{I}_d)$.

Model A.3. Mixture of the d -variate normal distribution with mixing probability 0.8, where the samples are taken as a from $0.8N_d(\mathbf{0}_d, \mathbf{I}_d) + 0.2N_d(\mathbf{0}_d, \Sigma)$. Here, Σ be a compound symmetric matrix with off-diagonal elements as 0.5 and diagonal elements as 1.

Model A.4. d -variate t-distribution with degrees of freedom 3, $t(\mathbf{0}_d, \mathbf{I}_d, 3)$.

Model A.5. Standard d -variate Cauchy distribution $C(\mathbf{0}_d, \mathbf{I}_d)$ or $t(\mathbf{0}_d, \mathbf{I}_d, 1)$ with p.d.f. $f(\mathbf{x}) = [\Gamma((d+1)/2)/(\sqrt{\pi}\Gamma(d/2))] \times (1 + \|\mathbf{x}\|^2)^{-(d+1)/2}$.

Model A.6. Standard d -variate Laplace distribution $L(\mathbf{0}_d, \mathbf{I}_d)$ with p.d.f. $f(\mathbf{x}) = [\Gamma(d/2)/(2\Gamma(d)\pi^{d/2})] \times \exp(-\|\mathbf{x}\|)$.

We fix the sample size $n \in \{10, 25, 50, 100, 300, 500\}$ and the nominal significance level α is assumed to be 0.05. We compare the proposed method denoted as KS.depth and CvM.depth respectively with Anderson-Darling (AD), Cramér-von Mises (CvM), Doornik-Hansen (DH), Henze-Zirkler (HZ), Royston (R) tests and a series of χ^2 -type

tests such as McCulloch (M), Nikulin-Rao-Robson (NRR), Dzhaparidze-Nikulin (DN) tests.

Tables 1, 2 and 3 describe Monte Carlo results for goodness-of-fit tests that represents the observed relative frequency for rejecting H_0 for $d = 2, 6$ and 10 respectively. Here, the observed relative frequency for rejecting the null for Model A.1 indicates the size of the test and for Model A.2-A.6 represent the power of the test for different alternatives. If we increase the sample size n the power of the test increases for all the methods and the size of the test are more or less stabilized at the nominal significance level. If we increase the dimension of the data, the aforementioned statement holds true. The power of the proposed tests are consistently better for all the choices of alternative distributions. Moreover, for mixture distributions like Model A.2 and A.3, the competing testing procedures are worse, whereas the proposed methods KS.depth and CvM.depth perform satisfactorily. The Figure 5 represents receiver operating characteristics (ROC) curve that illustrates the performance of testing procedure. The ROC curve is created by plotting the power as a function of the Type I error of the testing procedure. For brevity, here we represent the ROC curve for the goodness-of-fit test when the alternative hypotheses are (a) Cauchy and (d) Laplace distributions for small sample size. Here, this figure tells us that our proposed testing procedures (especially the data-depth based CvM method) outperform the existing methods.

In the two-sample test scenario (see Problem 2), we use sample sizes (n, m) such that $\rho = n/(n + m) \in \{0.3, 0.5, 0.8\}$ and fix $n \in \{50, 100, 300\}$. We generate samples from the following distribution family.

Model B. The first samples are taken from the standard multivariate distribution $N_d(\mathbf{0}_d, \mathbf{I}_d)$ and the second sample is taken from the d variate normal $N_d(\mu \times \mathbf{1}_d, \mathbf{I}_d)$ where we chose $\mu \in \{0, 0.5, 01\}$.

Table 4 represents the observed relative frequency for rejecting H_0 based on the above model. The values on the table corresponding to $\mu = 0$ is the size of the test and that to $\mu = \mu_0 \in \{0.5, 1\}$ represent the power of the test at μ_0 . If μ creases, so do the powers of the tests. Even if the dimension of the data is increased, the performance of the proposed test is not affected.

Table 1: Goodness-of-fit test: Observed relative frequency for rejecting the null, $d = 2$.

n	KS.depth	CvM.depth	AD	CM	DH	HZ	R	McCulloch	NRR	DN
Model A.1. $H_0 : \mathbf{X} \sim N_2(\mathbf{0}_2, \mathbf{I}_2)$ against $H_1 : \mathbf{X} \sim N_2(\mathbf{0}_2, \mathbf{I}_2)$										
10	0.074	0.040	0.060	0.050	0.052	0.020	0.040	0.032	0.050	0.062
25	0.040	0.028	0.034	0.030	0.044	0.052	0.044	0.030	0.044	0.054
50	0.038	0.056	0.060	0.058	0.060	0.042	0.056	0.044	0.048	0.048
100	0.052	0.058	0.042	0.056	0.048	0.046	0.044	0.044	0.060	0.062
300	0.055	0.090	0.060	0.055	0.065	0.050	0.055	0.080	0.055	0.050
500	0.070	0.066	0.052	0.050	0.072	0.038	0.060	0.038	0.064	0.054
Model A.2. $H_0 : \mathbf{X} \sim N_2(\mathbf{0}_2, \mathbf{I}_2)$ against $H_1 : \mathbf{X} \sim 0.8N_2(\mathbf{0}_2, \mathbf{I}_2) + 0.2N_2(5\mathbf{1}_2, \mathbf{I}_2)$										
10	0.600	0.800	0.000	0.000	0.000	0.000	0.600	0.000	0.200	0.200
25	0.751	0.788	0.168	0.157	0.129	0.980	0.996	0.105	0.122	0.090
50	0.886	0.930	0.212	0.214	0.198	1.000	1.000	0.144	0.158	0.122
100	0.994	1.000	0.328	0.334	0.488	1.000	1.000	0.118	0.250	0.224
300	1.000	1.000	0.656	0.662	0.982	1.000	1.000	0.134	0.668	0.684
500	1.000	1.000	0.810	0.818	1.000	1.000	1.000	0.132	0.832	0.822
Model A.3. $H_0 : \mathbf{X} \sim N_2(\mathbf{0}_2, \mathbf{I}_2)$ against $H_1 : \mathbf{X} \sim 0.8N_2(\mathbf{0}_2, \mathbf{I}_2) + 0.2N_2(\mathbf{0}_2, \Sigma)$										
10	0.600	0.600	0.400	0.200	0.200	0.000	0.200	0.200	0.200	0.200
25	0.469	0.611	0.050	0.035	0.048	0.046	0.050	0.046	0.046	0.066
50	0.532	0.650	0.052	0.042	0.056	0.056	0.054	0.036	0.048	0.040
100	0.588	0.732	0.046	0.050	0.054	0.048	0.040	0.048	0.050	0.056
300	0.644	0.808	0.082	0.068	0.064	0.078	0.060	0.064	0.068	0.056
500	0.690	0.844	0.054	0.060	0.062	0.052	0.064	0.084	0.048	0.040
Model A.4. $H_0 : \mathbf{X} \sim N_2(\mathbf{0}_2, \mathbf{I}_2)$ against $H_1 : \mathbf{X} \sim t(\mathbf{0}_2, \mathbf{I}_2, 3)$										
10	0.296	0.300	0.104	0.072	0.172	0.176	0.178	0.026	0.040	0.054
25	0.412	0.600	0.478	0.444	0.524	0.462	0.456	0.396	0.356	0.174
50	0.702	0.900	0.822	0.818	0.822	0.772	0.758	0.788	0.756	0.430
100	0.956	0.994	0.994	0.992	0.986	0.978	0.972	0.988	0.986	0.810
300	1.000	1.000	1.000	1.000	1.000	1.000	1.000	1.000	1.000	1.000
500	1.000	1.000	1.000	1.000	1.000	1.000	1.000	1.000	1.000	1.000
Model A.5. $H_0 : \mathbf{X} \sim N_2(\mathbf{0}_2, \mathbf{I}_2)$ against $H_1 : \mathbf{X} \sim C(\mathbf{0}_2, \mathbf{I}_2)$										
10	0.728	0.790	0.476	0.438	0.588	0.708	0.550	0.190	0.258	0.234
25	0.974	0.988	0.982	0.974	0.954	0.988	0.960	0.922	0.948	0.860
50	1.000	1.000	1.000	1.000	1.000	1.000	1.000	0.998	1.000	0.996
100	1.000	1.000	1.000	1.000	1.000	1.000	1.000	1.000	1.000	1.000
300	1.000	1.000	1.000	1.000	1.000	1.000	1.000	1.000	1.000	1.000
500	1.000	1.000	1.000	1.000	1.000	1.000	1.000	1.000	1.000	1.000
Model A.6. $H_0 : \mathbf{X} \sim N_2(\mathbf{0}_2, \mathbf{I}_2)$ against $H_1 : \mathbf{X} \sim L(\mathbf{0}_2, \mathbf{I}_2)$										
10	0.272	0.252	0.116	0.078	0.194	0.158	0.168	0.022	0.040	0.066
25	0.422	0.670	0.550	0.474	0.520	0.520	0.458	0.260	0.302	0.224
50	0.720	0.960	0.908	0.882	0.786	0.842	0.752	0.622	0.738	0.514
100	0.946	0.998	0.992	0.992	0.950	0.992	0.934	0.914	0.980	0.878
300	1.000	1.000	1.000	1.000	1.000	1.000	1.000	1.000	1.000	1.000
500	1.000	1.000	1.000	1.000	1.000	1.000	1.000	1.000	1.000	1.000

Table 2: Goodness-of-fit test: Observed relative frequency for rejecting the null, $d = 6$.

n	KS.depth	CvM.depth	AD	CM	DH	HZ	R	McCulloch	NRR	DN
Model A.1. $H_0 : \mathbf{X} \sim N_6(\mathbf{0}_6, \mathbf{I}_6)$ against $H_1 : \mathbf{X} \sim N_6(\mathbf{0}_6, \mathbf{I}_6)$										
10	0.072	0.042	0.066	0.062	0.054	0.004	0.060	0.008	0.376	0.610
25	0.066	0.052	0.050	0.070	0.050	0.030	0.034	0.046	0.084	0.092
50	0.064	0.052	0.060	0.052	0.034	0.038	0.034	0.048	0.060	0.066
100	0.046	0.050	0.056	0.066	0.044	0.046	0.036	0.064	0.070	0.068
300	0.039	0.072	0.083	0.072	0.056	0.028	0.050	0.050	0.061	0.078
500	0.038	0.068	0.038	0.038	0.050	0.060	0.062	0.048	0.046	0.044
Model A.2. $H_0 : \mathbf{X} \sim N_6(\mathbf{0}_6, \mathbf{I}_6)$ against $H_1 : \mathbf{X} \sim 0.8N_6(\mathbf{0}_6, \mathbf{I}_6) + 0.2N_6(5\mathbf{1}_6, \mathbf{I}_6)$										
10	0.941	1.000	0.059	0.000	0.059	0.000	0.706	0.000	0.412	0.529
25	1.000	1.000	0.083	0.083	0.042	0.292	1.000	0.042	0.083	0.125
50	0.996	1.000	0.048	0.040	0.068	0.920	1.000	0.064	0.054	0.064
100	1.000	1.000	0.094	0.086	0.088	1.000	1.000	0.084	0.096	0.082
300	1.000	1.000	0.150	0.136	0.130	1.000	1.000	0.054	0.104	0.106
500	1.000	1.000	0.234	0.186	0.184	1.000	1.000	0.050	0.140	0.150
Model A.3. $H_0 : \mathbf{X} \sim N_6(\mathbf{0}_6, \mathbf{I}_6)$ against $H_1 : \mathbf{X} \sim 0.8N_6(\mathbf{0}_6, \mathbf{I}_6) + 0.2N_6(\mathbf{0}_6, \Sigma)$										
10	0.882	1.000	0.059	0.059	0.059	0.000	0.059	0.000	0.176	0.529
25	0.958	1.000	0.042	0.042	0.000	0.000	0.000	0.042	0.000	0.083
50	0.910	0.962	0.032	0.036	0.064	0.046	0.044	0.038	0.060	0.060
100	0.930	0.970	0.054	0.054	0.040	0.088	0.044	0.044	0.056	0.052
300	0.952	0.986	0.152	0.124	0.046	0.092	0.044	0.090	0.078	0.068
500	0.976	0.992	0.300	0.240	0.074	0.152	0.050	0.158	0.168	0.124
Model A.4. $H_0 : \mathbf{X} \sim N_6(\mathbf{0}_6, \mathbf{I}_6)$ against $H_1 : \mathbf{X} \sim t(\mathbf{0}_6, \mathbf{I}_6, 3)$										
10	0.116	0.154	0.018	0.016	0.080	0.054	0.066	0.056	0.240	0.354
25	0.640	0.836	0.646	0.492	0.572	0.742	0.470	0.272	0.404	0.284
50	0.904	0.994	0.996	0.994	0.966	0.994	0.908	0.924	0.980	0.860
100	0.994	1.000	1.000	1.000	1.000	1.000	0.998	1.000	1.000	1.000
300	1.000	1.000	1.000	1.000	1.000	1.000	1.000	1.000	1.000	1.000
500	1.000	1.000	1.000	1.000	1.000	1.000	1.000	1.000	1.000	1.000
Model A.5. $H_0 : \mathbf{X} \sim N_6(\mathbf{0}_6, \mathbf{I}_6)$ against $H_1 : \mathbf{X} \sim C(\mathbf{0}_6, \mathbf{I}_6)$										
10	0.308	0.498	0.024	0.004	0.146	0.314	0.124	0.308	0.162	0.078
25	0.998	0.998	0.996	0.992	0.990	0.998	0.968	0.880	0.976	0.946
50	1.000	1.000	1.000	1.000	1.000	1.000	1.000	0.998	1.000	1.000
100	1.000	1.000	1.000	1.000	1.000	1.000	1.000	1.000	1.000	1.000
300	1.000	1.000	1.000	1.000	1.000	1.000	1.000	1.000	1.000	1.000
500	1.000	1.000	1.000	1.000	1.000	1.000	1.000	1.000	1.000	1.000
Model A.6. $H_0 : \mathbf{X} \sim N_6(\mathbf{0}_6, \mathbf{I}_6)$ against $H_1 : \mathbf{X} \sim L(\mathbf{0}_6, \mathbf{I}_6)$										
10	0.114	0.168	0.024	0.014	0.084	0.100	0.076	0.084	0.294	0.344
25	0.656	0.912	0.828	0.590	0.568	0.896	0.438	0.080	0.400	0.418
50	0.910	0.996	1.000	0.990	0.942	1.000	0.854	0.682	0.966	0.930
100	1.000	1.000	1.000	1.000	1.000	1.000	1.000	0.982	1.000	1.000
300	1.000	1.000	1.000	1.000	1.000	1.000	1.000	1.000	1.000	1.000
500	1.000	1.000	1.000	1.000	1.000	1.000	1.000	1.000	1.000	1.000

Table 3: Goodness-of-fit test: Observed relative frequency for rejecting the null, $d = 10$.

n	KS.depth	CvM.depth	AD	CM	DH	HZ	R	McCulloch	NRR	DN
Model A.1. $H_0 : \mathbf{X} \sim N_{10}(\mathbf{0}_{10}, \mathbf{I}_{10})$ against $H_1 : \mathbf{X} \sim N_{10}(\mathbf{0}_{10}, \mathbf{I}_{10})$										
25	0.050	0.050	0.038	0.042	0.038	0.028	0.050	0.034	0.158	0.168
50	0.052	0.042	0.036	0.040	0.066	0.040	0.052	0.060	0.088	0.092
100	0.054	0.062	0.050	0.052	0.052	0.052	0.052	0.056	0.080	0.078
300	0.040	0.023	0.051	0.040	0.069	0.069	0.057	0.057	0.040	0.040
500	0.050	0.060	0.058	0.052	0.056	0.054	0.060	0.042	0.048	0.050
Model A.2. $H_0 : \mathbf{X} \sim N_{10}(\mathbf{0}_{10}, \mathbf{I}_{10})$ against $H_1 : \mathbf{X} \sim 0.8N_{10}(\mathbf{0}_{10}, \mathbf{I}_{10}) + 0.2N_{10}(5\mathbf{1}_{10}, \mathbf{I}_{10})$										
25	0.995	0.997	0.032	0.037	0.037	0.099	1.000	0.048	0.136	0.171
50	0.998	1.000	0.042	0.042	0.062	0.330	1.000	0.072	0.096	0.094
100	1.000	1.000	0.051	0.042	0.051	0.850	1.000	0.060	0.066	0.060
300	1.000	1.000	0.050	0.054	0.082	1.000	1.000	0.046	0.070	0.080
500	1.000	1.000	0.093	0.086	0.064	1.000	1.000	0.061	0.068	0.068
Model A.3. $H_0 : \mathbf{X} \sim N_{10}(\mathbf{0}_{10}, \mathbf{I}_{10})$ against $H_1 : \mathbf{X} \sim 0.8N_{10}(\mathbf{0}_{10}, \mathbf{I}_{10}) + 0.2N_{10}(\mathbf{0}_{10}, \Sigma)$										
25	0.979	1.000	0.019	0.024	0.051	0.043	0.043	0.061	0.131	0.120
50	0.976	1.000	0.014	0.010	0.060	0.052	0.060	0.032	0.032	0.034
100	0.978	0.996	0.040	0.028	0.068	0.078	0.054	0.068	0.060	0.056
300	0.934	0.986	0.288	0.212	0.074	0.160	0.056	0.084	0.120	0.128
500	0.894	0.982	0.548	0.430	0.068	0.310	0.054	0.122	0.260	0.238
Model A.4. $H_0 : \mathbf{X} \sim N_{10}(\mathbf{0}_{10}, \mathbf{I}_{10})$ against $H_1 : \mathbf{X} \sim t(\mathbf{0}_{10}, \mathbf{I}_{10}, 3)$										
25	0.330	0.708	0.296	0.098	0.384	0.676	0.272	0.054	0.160	0.198
50	0.830	0.996	1.000	0.990	0.978	1.000	0.912	0.886	0.974	0.922
100	0.998	1.000	1.000	1.000	1.000	1.000	1.000	1.000	1.000	1.000
300	1.000	1.000	1.000	1.000	1.000	1.000	1.000	1.000	1.000	1.000
500	1.000	1.000	1.000	1.000	1.000	1.000	1.000	1.000	1.000	1.000
Model A.5. $H_0 : \mathbf{X} \sim N_{10}(\mathbf{0}_{10}, \mathbf{I}_{10})$ against $H_1 : \mathbf{X} \sim C(\mathbf{0}_{10}, \mathbf{I}_{10})$										
25	0.930	0.996	0.970	0.904	0.908	0.998	0.844	0.092	0.848	0.854
50	1.000	1.000	1.000	1.000	1.000	1.000	1.000	0.998	1.000	1.000
100	1.000	1.000	1.000	1.000	1.000	1.000	1.000	1.000	1.000	1.000
300	1.000	1.000	1.000	1.000	1.000	1.000	1.000	1.000	1.000	1.000
500	1.000	1.000	1.000	1.000	1.000	1.000	1.000	1.000	1.000	1.000
Model A.6. $H_0 : \mathbf{X} \sim N_{10}(\mathbf{0}_{10}, \mathbf{I}_{10})$ against $H_1 : \mathbf{X} \sim L(\mathbf{0}_{10}, \mathbf{I}_{10})$										
25	0.436	0.900	0.740	0.312	0.446	0.948	0.328	0.224	0.470	0.394
50	0.894	1.000	1.000	0.998	0.950	1.000	0.890	0.430	0.968	0.966
100	1.000	1.000	1.000	1.000	1.000	1.000	0.998	0.978	1.000	1.000
300	1.000	1.000	1.000	1.000	1.000	1.000	1.000	1.000	1.000	1.000
500	1.000	1.000	1.000	1.000	1.000	1.000	1.000	1.000	1.000	1.000

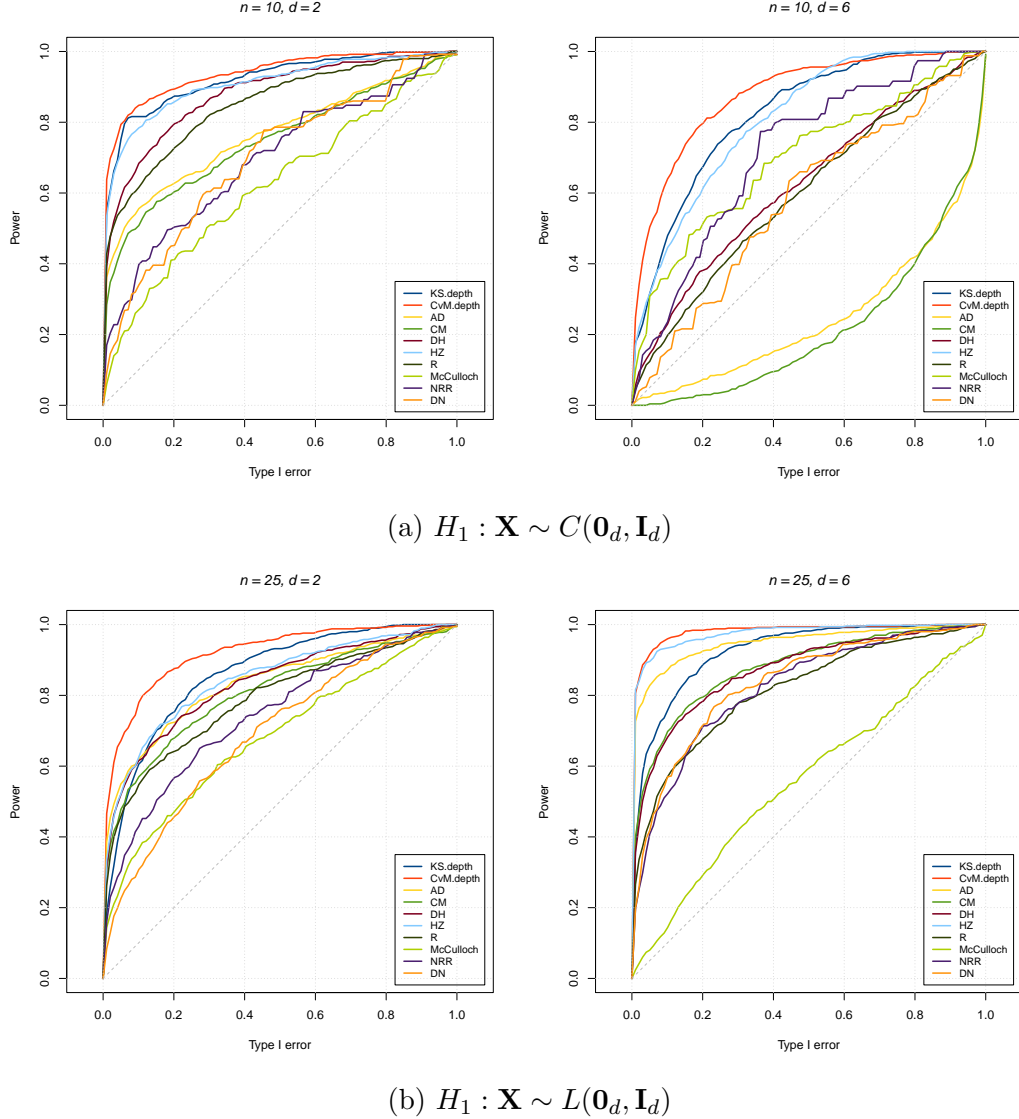


Figure 5: ROC plot for the goodness-of-fit test when the alternative distributions are standard Cauchy (a) and standard Laplace distribution (b), respectively, where the null distribution is standard normal distribution.

Table 4: Two-sample test: Observed relative frequency for rejecting the null based on Model B.

	n	m	$\mu = 0$		$\mu = 0.5$		$\mu = 1$	
			KS.depth	CvM.depth	KS.depth	CvM.depth	KS.depth	CvM.depth
<i>d</i> = 2								
	50	117	0.054	0.052	0.908	0.940	1.000	1.000
$\rho = 0.3$	100	234	0.050	0.058	0.994	0.998	1.000	1.000
	300	700	0.061	0.046	1.000	1.000	1.000	1.000
	50	50	0.064	0.064	0.790	0.836	0.998	1.000
$\rho = 0.5$	100	100	0.066	0.068	0.974	0.986	1.000	1.000
	300	300	0.048	0.058	1.000	1.000	1.000	1.000
	50	13	0.092	0.076	0.416	0.452	0.904	0.926
$\rho = 0.8$	100	25	0.064	0.060	0.676	0.780	0.996	1.000
	300	75	0.058	0.054	0.996	0.998	1.000	1.000
<i>d</i> = 6								
	50	117	0.072	0.070	0.996	0.986	1.000	1.000
$\rho = 0.3$	100	234	0.074	0.064	1.000	1.000	1.000	1.000
	300	700	0.056	0.060	1.000	1.000	1.000	1.000
	50	50	0.132	0.058	0.998	0.996	1.000	1.000
$\rho = 0.5$	100	100	0.052	0.052	1.000	1.000	1.000	1.000
	300	300	0.048	0.056	1.000	1.000	1.000	1.000
	50	13	0.290	0.206	0.914	0.892	0.986	0.998
$\rho = 0.8$	100	25	0.132	0.102	0.976	0.988	1.000	1.000
	300	75	0.068	0.064	1.000	1.000	1.000	1.000
<i>d</i> = 10								
	50	117	0.086	0.078	1.000	0.997	1.000	1.000
$\rho = 0.3$	100	234	0.066	0.070	1.000	1.000	1.000	1.000
	300	700	0.031	0.073	1.000	1.000	1.000	1.000
	50	50	0.106	0.048	1.000	1.000	1.000	1.000
$\rho = 0.5$	100	100	0.068	0.062	1.000	1.000	1.000	1.000
	300	300	0.052	0.050	1.000	1.000	1.000	1.000
	50	13	0.486	0.264	0.976	0.976	0.990	0.996
$\rho = 0.8$	100	25	0.140	0.116	1.000	0.998	1.000	1.000
	300	75	0.066	0.064	1.000	1.000	1.000	1.000

6 Real data analysis

To understand the practicability of the proposed tests, two well-known data sets are analyzed here.

Fisher's *Iris* data

This data set, available in the base R, consists of three multivariate samples corresponding to three different species of Iris, namely *Iris setosa*, *Iris virginica* and *Iris versicolor* with sample size 50 for each species. In each species, the length and width of the sepals are measured in centimeters. We would like to determine how close the distribution of each sample associated with sepal length and sepal width is to a bivariate normal sample. This can be formulated as a goodness-of-fit testing problem, with F_0 being a bivariate normal distribution with unknown mean μ and unknown dispersion matrix Σ . For each species, we estimate these unknown parameters using the corresponding mean vector and covariance matrix. The data-depth discrepancy is graphically represented for three different species in Figure 6, where we observe that most points are tightly clustered around the straight line, indicating that the standardized data are from a standard bivariate normal distribution. Moreover, our goodness-of-fit test for testing $H_0 : F = F_0$ against $H_1 : F \neq F_0$ led to very high empirical p-values for all types of species (see Table 5). This indicates that H_0 is to be accepted, and therefore, bivariate normal distributions show signs of good fit for the data for the sepal length and sepal width of three Iris species.

Table 5: Empirical p-values of the proposed goodness-of-fit tests obtained over 1000 replications.

Species	p-value of depth based tests	
	KS.depth	CvM.depth
<i>Iris setosa</i>	0.286	0.418
<i>Iris virginica</i>	0.43	0.39
<i>Iris versicolor</i>	0.19	0.118

gilgais data

This data set is available in the MASS package in R. It is collected on a line transect survey in the gilgai territory in New South Wales, Australia (Webster, 1977).

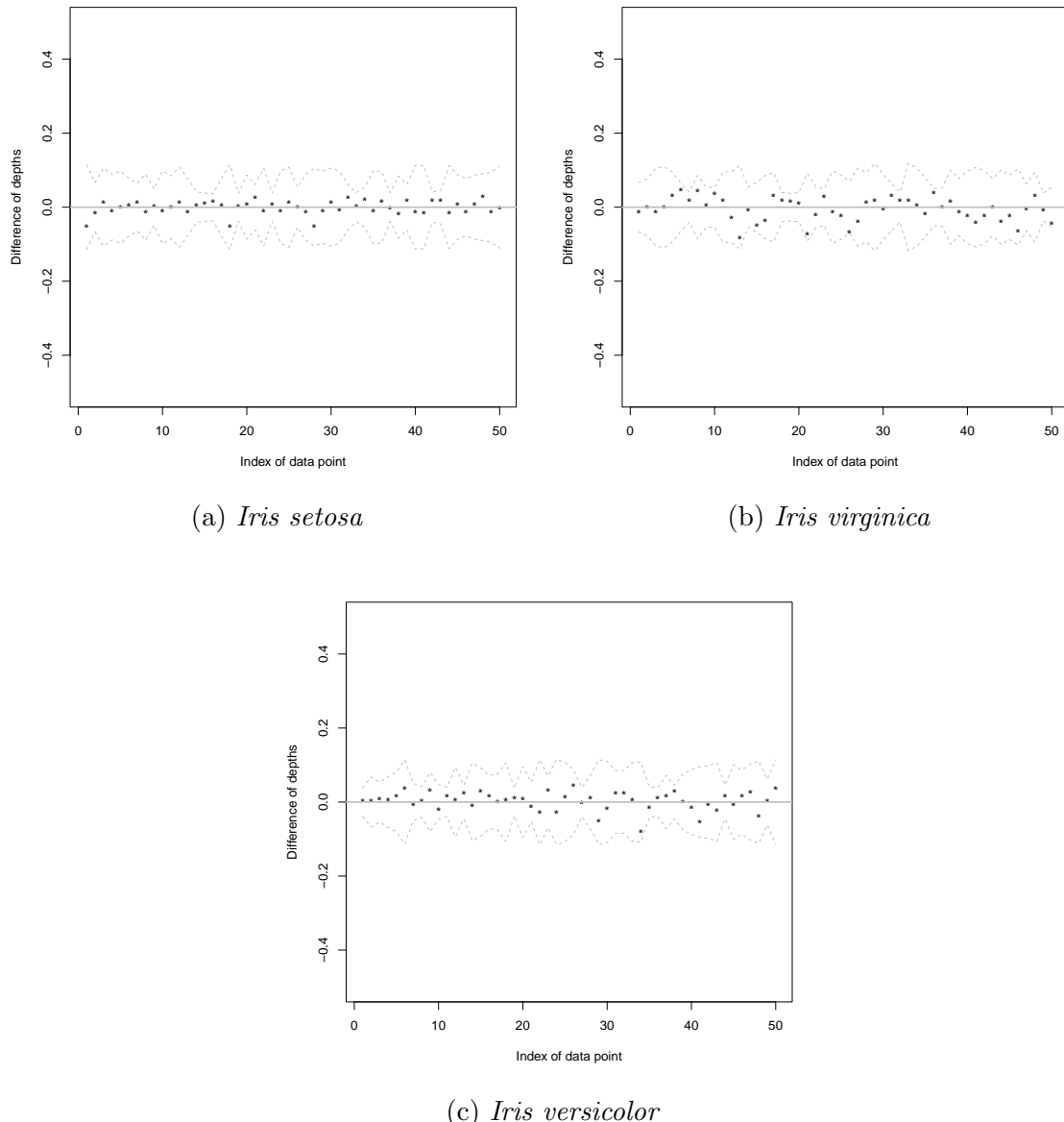


Figure 6: *Goodness-of-fit test for Iris data*: The data-depth discrepancy plot for *Iris setosa*, *Iris virginica* and *Iris versicolor* respectively for testing normality. The dotted gray curves indicate the two-sigma limits of data-depth discrepancy

On a 4-meter spaced linear grid, 365 sampling locations are selected. Electrical conductivity (in mS / cm), pH, and chloride contained (in ppm) are collected at three different depths below the surface, 0-10 cm, 30-40 cm, and 80-90 cm. We would like to investigate how close the joint distribution of three variables at each level is to a trivariate normal distribution. As the previous example, this can be formulated as a goodness-of-fit problem, where F_0 is specified as a trivariate normal distribution with unknown mean μ and unknown dispersion matrix Σ . We estimate these unknown parameters using their respective maximum likelihood estimates. We then standardize the data in each sample using the corresponding mean vector and covariance matrix. The proposed data-depth dispersion plot is shown in Figure 7 where we observe a majority of the data cloud is far from the straight line. This phenomenon indicates that the data are not from a trivariate normal distribution. Moreover, the test of $H_0 : F = F_0$ against $H_1 : F \neq F_0$ led to zero empirical p-values for all height levels below the surface. Moreover, we are interested to study whether distribution of any height is same as the other. Therefore, this can be viewed as two-sample test where F is the distribution of chemical parameters at height at 0 – 10 cm and G is that of either at height 30–40 cm or 80–90 cm, respectively. The Figure 8b shows that the data cloud is far from the straight line, this phenomenon indicates that the distributions are different. Moreover, the empirical p-value for each of situations are close to zero based on the proposed test which determines that the distributions are significantly different.

7 Conclusion

In this paper, we have proposed a data-depth discrepancy and a graphical toolkit based on Tukey’s half-space depth. This device is used to test the equality of two distribution functions and is applicable to any dimension of the distributions. The motivations behind the graphical device are shown through simulation examples. Influenced by the graphical device, we have proposed test statistics based on the Kolmogorov-Smirnov and Cramér-von Mises tests. For goodness-of-fit and two-sample testing problems, the proposed test statistics can test the equality of two distribution functions, which are common in practice. We have shown that the test statistics are point-wise and also uniformly constant. Moreover, we have studied the asymptotic power under contiguous alternatives. The applicability of the proposed

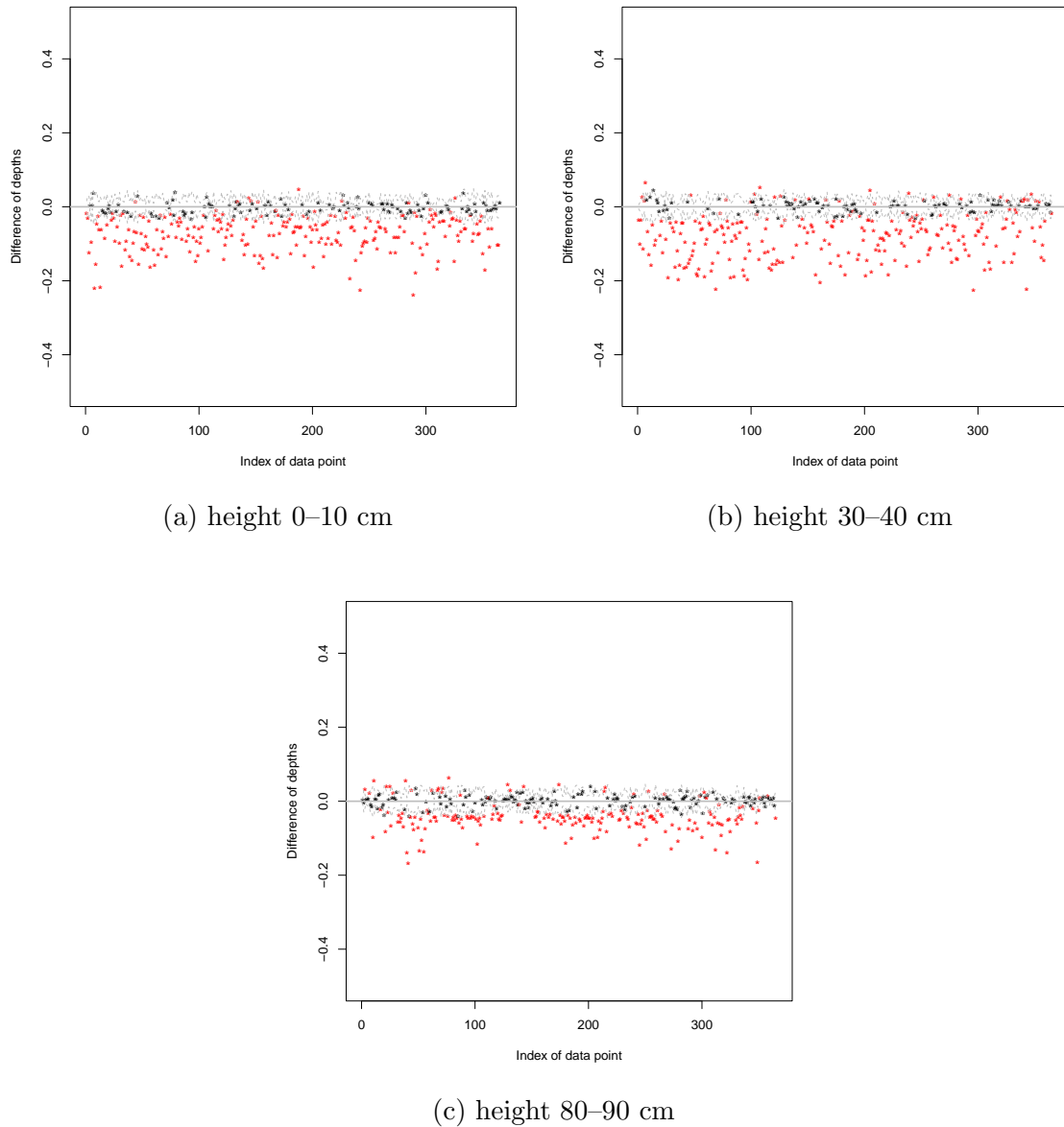


Figure 7: Goodness-of-fit test for gilgais data: The data-depth discrepancy plot for tuple at depths below the surface of height 0-10 cm, 30-40 cm and 80-90 cm respectively for testing normality. The dotted gray curves indicate the two-sigma limits of data-depth discrepancy

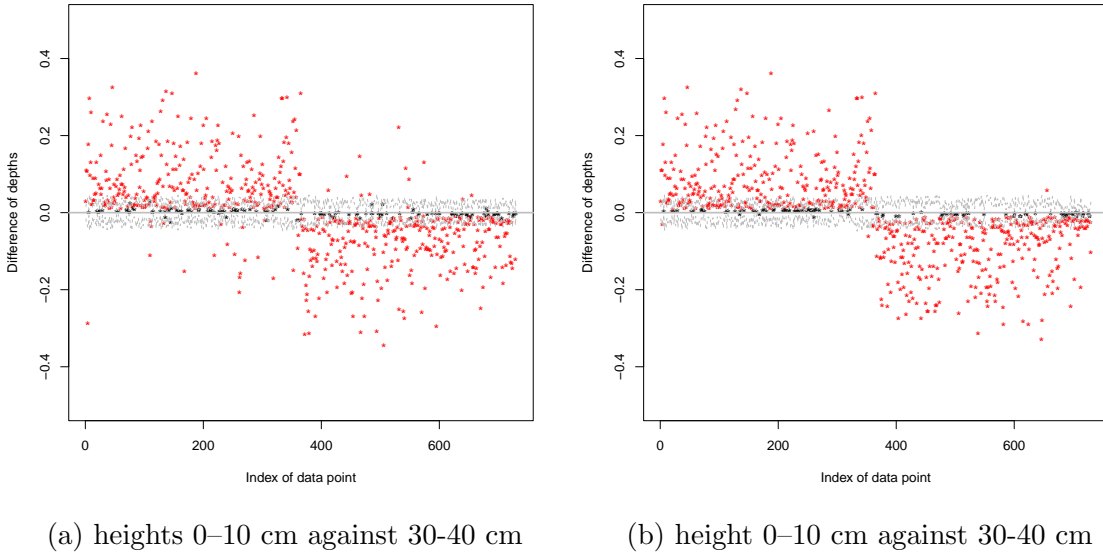


Figure 8: Two-sample test for gilgias data: The data-depth discrepancy plot for heights 0–10 cm against 30–40 cm and height 0–10 cm against 30–40 cm are shown. The dotted gray curves indicate the two-sigma limits of data-depth discrepancy

method is illustrated by simulation studies and real data analysis. The graphical tool and test statistics developed in this article can be used regardless of the dimension of the data and therefore, significantly contributes to statistics and machine learning literature.

Acknowledgement : Subhra Sankar Dhar is thankful to the research grants MTR/2019/000039 and CRG/2022/001489, Government of India.

Appendix

Proof of Theorem 1.

Note that, for every $\epsilon > 0$,

$$\lim_{n \rightarrow \infty} \mathbb{P} \left\{ \widehat{\mathcal{C}}(\mathcal{X}, F_0) \subset \mathcal{C}_\epsilon(F, F_0) \right\} \geq \mathbb{P} \left\{ \sup_{\mathbf{x}} |D_{\mathcal{X}}(\mathbf{x}) - D_{F_0}(\mathbf{x})| < \epsilon \right\} \rightarrow 1 \quad (18)$$

due to the Proposition 4.4 of Massé (2004). \square

Proof of Theorem 2.

By the similar argument of Theorem 2, using the fact that $\lim_{\min(n,m) \rightarrow \infty} n/(n+m) = \lambda \in (0, 1)$, observe that,

$$\lim_{\min(n,m) \rightarrow \infty} \mathbb{P}\{\widehat{\mathcal{C}}(\mathcal{X}, \mathcal{Y}) \subset \mathcal{C}_\epsilon(F, G)\} \geq \mathbb{P}\left\{\sup_{\mathbf{x}} |D_{\mathcal{X}}(\mathbf{x}) - D_{\mathcal{Y}}(\mathbf{x})| < \epsilon\right\} \rightarrow 1$$

□

Proof of Theorem 3.

Let us define the Kolmogorov-Smirnov distance between empirical and theoretical distribution functions \widehat{F}_n and F_0 based on Tukey's half-space depth D as $d_K(\mathcal{X}, F_0) = \sup_{\mathbf{x} \in \mathbb{R}^d} |D_{\mathcal{X}}(\mathbf{x}) - D_{F_0}(\mathbf{x})| = \sup_{\mathbf{x}, \mathbf{u}} |\widehat{F}_n(H[\mathbf{x}, \mathbf{u}]) - F_0(H[\mathbf{x}, \mathbf{u}])|$ where $\mathcal{X} = \{\mathbf{X}_1, \dots, \mathbf{X}_n\}$ and H is the half-space with $H[\mathbf{x}, \mathbf{u}] = \{\mathbf{y} \in \mathbb{R}^d : \mathbf{u}^T \mathbf{x} \geq \mathbf{u}^T \mathbf{y}\}$. It is important to note that $d_K(\cdot, \cdot)$ has the Glivenko-Cantelli property (Pollard, 1984; Donoho and Gasko, 1992), i.e., if the data samples are i.i.d. from F_0 , $d_K(\mathcal{X}, F_0) \rightarrow 0$ as $n \rightarrow \infty$. Therefore, under an alternative F , we have

$$\sup_{\mathbf{x}} |D_{\mathcal{X}}(\mathbf{x}) - D_{F_0}(\mathbf{x})| \rightarrow d_K(D_F, D_{F_0}) > 0 \quad (19)$$

almost surely. Now fix any F with $d_K(D_F, D_{F_0}) > 0$, then there exists some \mathbf{x} with $D_{\mathcal{X}}(\mathbf{x}) \neq D_F(\mathbf{x})$. Without loss of generality, assume that $D_{\mathcal{X}}(\mathbf{x}) > D_{F_0}(\mathbf{x})$. Then

$$\begin{aligned} \mathbb{P}_F \left\{ T_{\mathcal{X}, F_0}^{\text{KS}} > s_{1-\alpha}^{(1)} \right\} &\geq \mathbb{P}_F \left\{ \sqrt{n} |D_{\mathcal{X}}(\mathbf{x}) - D_{F_0}(\mathbf{x})| > s_{1-\alpha}^{(1)} \right\} \\ &= \mathbb{P}_F \left\{ \sqrt{n} [D_{\mathcal{X}}(\mathbf{x}) - D_F(\mathbf{x}) + D_F(\mathbf{x}) - D_{F_0}(\mathbf{x})] > s_{1-\alpha}^{(1)} \right\} \\ &\geq \mathbb{P}_F \left\{ \sqrt{n} [D_{\mathcal{X}}(\mathbf{x}) - D_F(\mathbf{x})] > s_{1-\alpha}^{(1)} - \sqrt{n} [D_F(\mathbf{x}) - D_{F_0}(\mathbf{x})] \right\} \\ &\rightarrow 1 \text{ as } n \rightarrow \infty. \end{aligned} \quad (20)$$

The last implication follows from the fact that $\{\sqrt{n}(D_{\mathcal{X}}(\mathbf{x}) - D_F(\mathbf{x}))\}$ is uniformly bounded in probability in view of Proposition 4 and an application of Prokhorov's theorem, and for finite $s_{1-\alpha}^{(1)}$, we have $s_{1-\alpha}^{(1)} - \sqrt{n}|D_F(\mathbf{x}) - D_{F_0}(\mathbf{x})| \rightarrow -\infty$ as $n \rightarrow \infty$. Hence the limiting power is one when $D_F(\mathbf{x}) > D_{F_0}(\mathbf{x})$. Similar argument can show that the limiting power is one when $D_F(\mathbf{x}) < D_{F_0}(\mathbf{x})$ for some \mathbf{x} . Hence, the proof is complete. □

Proof of Theorem 4.

Due to the Glivenko-Cantalli property of $d_K(\cdot, \cdot)$, under an alternative F , 19 holds almost surely. Thus fix any F with $d_K(D_F, D_{F_0}) > 0$, then there exists some \mathbf{x} with $D_{\mathcal{X}}(\mathbf{x}) \neq D_F(\mathbf{x})$. Therefore, observe that

$$\begin{aligned} \mathbb{P}_F \left\{ T_{\mathcal{X}, F_0}^{\text{CvM}} > s_{1-\alpha}^{(2)} \right\} &= \mathbb{P}_F \left\{ n \int (D_{\mathcal{X}}(\mathbf{x}) - D_{F_0}(\mathbf{x}))^2 dF_0(\mathbf{x}) > s_{1-\alpha}^{(2)} \right\} \\ &\geq \mathbb{P}_F \left\{ n \int (D_{\mathcal{X}}(\mathbf{x}) - D_F(\mathbf{x}))^2 dF_0(\mathbf{x}) > s_{1-\alpha}^{(2)} - a_n + 2b_n \right\} \\ &\rightarrow 1 \text{ as } n \rightarrow \infty, \end{aligned} \quad (21)$$

where $a_n = n \int (D_F(\mathbf{x}) - D_{F_0}(\mathbf{x}))^2 dF_0(\mathbf{x})$ and $b_n = n \int (D_{\mathcal{X}}(\mathbf{x}) - D_F(\mathbf{x}))(D_F(\mathbf{x}) - D_{F_0}(\mathbf{x})) dF_0(\mathbf{x})$. The last implication follows from the following facts: (i) $\{\sqrt{n}(D_{\mathcal{X}}(\mathbf{x}) - D_F(\mathbf{x}))\}$ is uniformly bounded in probability in view of Proposition 4, (ii) $s_{1-\alpha}^{(2)}$ is positive finite, and (iii) $\sup_{\mathbf{x}} |D_{\mathcal{X}}(\mathbf{x}) - D_F(\mathbf{x})| \rightarrow 0$ as $n \rightarrow \infty$ under F almost surely (see Donoho and Gasko (1992) and Proposition 4.4 of Massé (2004)). An application of Prokhorov's theorem shows that the limiting power is one when $D_F(\mathbf{x}) > D_{F_0}(\mathbf{x})$. Similar argument can show that the limiting power is one when $D_F(\mathbf{x}) < D_{F_0}(\mathbf{x})$ for some \mathbf{x} . Hence, the proof is complete. \square

Proof of Theorem 5. Let F_n be any distribution function that satisfies $\sqrt{n}d_K(D_{F_n}, D_{F_0}) \geq \Delta_n$. By the triangle inequality, we have

$$d_K(D_{F_n}, D_{F_0}) \leq d_K(D_{F_n}, D_{\mathcal{X}}) + d_K(D_{\mathcal{X}}, D_{F_0}), \quad (22)$$

which implies $T_{\mathcal{X}, F_0}^{\text{KS}} \geq \Delta_n - \sqrt{n}d_K(D_{F_n}, D_{F_0})$. Therefore,

$$\begin{aligned} \mathbb{P}_{F_n} \left\{ T_{\mathcal{X}, F_0}^{\text{KS}} > s_{1-\alpha}^{(1)} \right\} &\geq \mathbb{P}_{F_n} \left\{ \Delta_n - \sqrt{n}d_K(D_{F_n}, D_{\mathcal{X}}) > s_{1-\alpha}^{(1)} \right\} \\ &\geq \mathbb{P}_{F_n} \left\{ \sqrt{n}d_K(D_{F_n}, D_{\mathcal{X}}) \leq \Delta_n - s_{1-\alpha}^{(1)} \right\} \\ &\rightarrow 1 \text{ as } n \rightarrow \infty. \end{aligned} \quad (23)$$

The last implication follows from the following facts: (i) $\{\sqrt{n}(D_{\mathcal{X}}(\mathbf{x}) - D_F(\mathbf{x}))\}$ is uniformly bounded under F_n in probability in view of Proposition 4 (ii) $\Delta_n \rightarrow \infty$, and (iii) $s_{1-\alpha}^{(1)}$ is positive and finite. An application of Prokhorov's theorem, we get $\mathbb{P}_{F_n} \left\{ T_{\mathcal{X}, F_0}^{\text{KS}} > s_{1-\alpha}^{(1)} \right\} \rightarrow 1$. \square

Proof of Theorem 6.

Let F_n be any distribution function satisfies $\sqrt{n}d_K(D_{F_n}, D_{F_0}) \geq \Delta_n$. Therefore, using the triangle inequality 22, we have

$$\begin{aligned} \mathbb{P}_{F_n} \left\{ T_{\mathcal{X}, F_0}^{\text{CvM}} > s_{1-\alpha}^{(2)} \right\} &\geq \mathbb{P}_{F_n} \left\{ \int \Delta_n^2 dF_0(\mathbf{x}) - n \int d_K^2(D_{F_n}, D_{\mathcal{X}}) dF_0(\mathbf{x}) > s_{1-\alpha}^{(2)} \right\} \\ &\geq \mathbb{P}_{F_n} \left\{ n \int d_K^2(D_{F_n}, D_{\mathcal{X}}) dF_0(\mathbf{x}) \leq \int \Delta_n^2 dF_0(\mathbf{x}) - s_{1-\alpha}^{(2)} \right\} \\ &\rightarrow 1 \text{ as } n \rightarrow \infty. \end{aligned} \tag{24}$$

The last implication follows from the the following fact: (i) $\{\sqrt{n}(D_{\mathcal{X}}(\mathbf{x}) - D_F(\mathbf{x}))\}$ is uniformly bounded under F_n in probability in view of Proposition 4 (ii) $\Delta_n \rightarrow \infty$, and (iii) $s_{1-\alpha}^{(2)}$ is positive and finite. An application of Prokhorov's theorem, we get $\mathbb{P}_{F_n} \left\{ T_{\mathcal{X}, F_0}^{\text{CvM}} > s_{1-\alpha}^{(2)} \right\} \rightarrow 1$. \square

Proof of Theorem 7.

Define $a_{n,m} = \sqrt{n+m} \times d_K(D_F, D_G) = \sqrt{n+m}|D_F(\mathbf{x}) - D_G(\mathbf{x})|$.

$$\begin{aligned} \mathbb{P}_{H_1} \left\{ T_{\mathcal{X}, \mathcal{Y}}^{\text{KS}} > t_{1-\alpha}^{(1)} \right\} &\geq \mathbb{P}_{H_1} \left\{ \sqrt{n+m}|D_{\mathcal{X}}(\mathbf{x}) - D_{\mathcal{Y}}(\mathbf{x})| > t_{1-\alpha}^{(1)} \right\} \\ &\geq \mathbb{P}_{H_1} \left\{ \sqrt{n+m}|D_{\mathcal{X}}(\mathbf{x}) - D_F(\mathbf{x})| + \sqrt{n+m}|D_{\mathcal{Y}}(\mathbf{x}) - D_G(\mathbf{x})| > t_{1-\alpha}^{(1)} - a_{n,m} \right\} \\ &\geq \mathbb{P}_{H_1} \left\{ \lambda^{-1/2}\sqrt{n}|D_{\mathcal{X}}(\mathbf{x}) - D_F(\mathbf{x})| + (1-\lambda)^{-1/2}\sqrt{m}|D_{\mathcal{Y}}(\mathbf{x}) - D_G(\mathbf{x})| > t_{1-\alpha}^{(1)} - a_{n,m} \right\} \\ &\rightarrow 1 \text{ as } \min(n, m) \rightarrow \infty. \end{aligned} \tag{25}$$

The last implication follows from the fact that $\{\sqrt{n}(D_{\mathcal{X}}(\mathbf{x}) - D_F(\mathbf{x}))\}$ and $\{\sqrt{m}(D_{\mathcal{Y}}(\mathbf{x}) - D_G(\mathbf{x}))\}$ are uniformly bounded in probability in view of Proposition 4, for finite $t_{\alpha}^{(1)}$, we have $\sqrt{n+m}|D_F(\mathbf{x}) - D_G(\mathbf{x})| \rightarrow \infty$ as $\min(n, m) \rightarrow \infty$. By an application of Prokhorov's theorem, we get $\mathbb{P}_{H_1} \left\{ T_{\mathcal{X}, \mathcal{Y}}^{\text{KS}} > t_{1-\alpha}^{(1)} \right\} \rightarrow 1$ as $\min(n, m) \rightarrow \infty$.

Furthermore,

$$\begin{aligned} \mathbb{P}_{H_1} \left\{ T_{\mathcal{X}, \mathcal{Y}}^{\text{CvM}} > t_{1-\alpha}^{(2)} \right\} &\geq \mathbb{P} \left\{ \lambda^{-1}n \int (D_{\mathcal{X}}(\mathbf{x}) - D_F(\mathbf{x}))^2 dH_{n,m}(\mathbf{x}) \right. \\ &\quad \left. > t_{1-\alpha}^{(2)} \right\} \end{aligned}$$

$$\begin{aligned}
& + (1 - \lambda)^{-1} n \int (D_{\mathcal{Y}}(\mathbf{x}) - D_G(\mathbf{x}))^2 dH_{n,m}(\mathbf{x}) > t_{1-\alpha}^{(2)} - a_{n,m}^* \Big\} \\
& \rightarrow 1 \text{ as } \min(n, m) \rightarrow \infty
\end{aligned} \tag{26}$$

where $a_{n,m}^* = a_{n,m} - 2b_{n,m} + 2c_{n,m} - 2d_{n,m}$ with

$$\begin{aligned}
a_{n,m} &= (n+m) \int (D_F(\mathbf{x}) - D_G(\mathbf{x}))^2 dH_{n,m}(\mathbf{x}) \\
b_{n,m} &= (n+m) \int (D_{\mathcal{X}}(\mathbf{x}) - D_F(\mathbf{x}))(D_{\mathcal{Y}}(\mathbf{x}) - D_G(\mathbf{x})) dH_{n,m}(\mathbf{x}) \\
c_{n,m} &= (n+m) \int (D_{\mathcal{X}}(\mathbf{x}) - D_F(\mathbf{x}))(D_F(\mathbf{x}) - D_G(\mathbf{x})) dH_{n,m}(\mathbf{x}) \\
d_{n,m} &= (n+m) \int (D_{\mathcal{Y}}(\mathbf{x}) - D_G(\mathbf{x}))(D_F(\mathbf{x}) - D_G(\mathbf{x})) dH_{n,m}(\mathbf{x})
\end{aligned}$$

The last implication follows from the following facts: (i) $\{\sqrt{n}(D_{\mathcal{X}}(\mathbf{x}) - D_F(\mathbf{x}))\}$ and $\{\sqrt{m}(D_{\mathcal{Y}}(\mathbf{x}) - D_G(\mathbf{x}))\}$ are uniformly bounded in probability in view of Proposition 4, (ii) $t_{1-\alpha}^{(1)}$ is positive finite, (iii) $\lambda = \lim_{\min(n,m) \rightarrow \infty} \frac{n}{n+m} = \lambda \in (0, 1)$, (iv) $H_{n,m} \rightarrow H$ almost surely, due to Glivenko-Cantalli's theorem, (iv) $a_{n,m} \rightarrow \infty$, $b_{n,m}, c_{n,m}$ and $d_{n,m}$ are finite (due to (i)-(iv)). Thus, with an application of Prokhorov's theorem, we get $\mathbb{P}_{H_1} \left\{ T_{\mathcal{X}, \mathcal{Y}}^{\text{CvM}} > t_{1-\alpha}^{(2)} \right\} \rightarrow 1$ as $\min(n, m) \rightarrow \infty$.

Let F_n and G_m be any distribution functions that satisfies $\sqrt{n+m}d_K(D_{F_n}, D_{G_m}) \geq \Delta_{n,m}$. By triangle inequality, we have

$$d_K(D_{F_n}, D_{G_m}) \leq d_K(D_{F_n}, D_{\mathcal{X}}) + d_K(D_{\mathcal{X}}, D_{\mathcal{Y}}) + d_K(D_{\mathcal{Y}}, D_{G_m}) \tag{27}$$

which implies $T_{\mathcal{X}, \mathcal{Y}}^{\text{KS}} \geq \Delta_{n,m} - \sqrt{n+m}d_K(D_{\mathcal{X}}, D_{F_n}) - \sqrt{n+m}d_K(D_{\mathcal{Y}}, D_{G_m})$. Therefore,

$$\begin{aligned}
& \mathbb{P}_{F_n, G_m} \left\{ T_{\mathcal{X}, \mathcal{Y}}^{\text{KS}} > t_{1-\alpha}^{(1)} \right\} \\
& \geq \mathbb{P}_{F_n, G_m} \left\{ \Delta_{n,m} - \sqrt{n+m}d_K(D_{\mathcal{X}}, D_{F_n}) - \sqrt{n+m}d_K(D_{\mathcal{Y}}, D_{G_m}) > t_{1-\alpha}^{(1)} \right\} \\
& \geq \mathbb{P}_{F_n, G_m} \left\{ \sqrt{n+m}d_K(D_{\mathcal{X}}, D_{F_n}) + \sqrt{n+m}d_K(D_{\mathcal{Y}}, D_{G_m}) \leq \Delta_{n,m} - t_{1-\alpha}^{(1)} \right\} \\
& \rightarrow 1 \text{ as } \min(n, m) \rightarrow \infty.
\end{aligned} \tag{28}$$

The last implication follows from the following facts: (i) $\{\sqrt{n}(D_{\mathcal{X}}(\mathbf{x}) - D_F(\mathbf{x}))\}$ and $\{\sqrt{m}(D_{\mathcal{Y}}(\mathbf{x}) - D_G(\mathbf{x}))\}$ are uniformly bounded in probability under F_n and G_m

respectively in the view of Proposition 4, (ii) $\lambda \in (0, 1)$ and $t_{1-\alpha}^{(1)}$ is positive finite. (iii) $\Delta_{n,m} \rightarrow \infty$. An application of Prokhorov's theorem, we get $\mathbb{P}_{F_n, G_m} \left\{ T_{\mathcal{X}, \mathcal{Y}}^{\text{KS}} > t_{1-\alpha}^{(1)} \right\} \rightarrow 1$ as $\min(n, m) \rightarrow \infty$.

Moreover, by the inequality 27,

$$\begin{aligned}
& \mathbb{P}_{F_n, G_m} \left\{ T_{\mathcal{X}, \mathcal{Y}}^{\text{CvM}} > s_{1-\alpha}^{(2)} \right\} \\
& \geq \mathbb{P}_{F_n, G_m} \left\{ \int \Delta_{n,m}^2 dH_{n,m}(\mathbf{x}) - (n+m) \int d_K^2(D_{\mathcal{X}}, D_{F_n}) dH_{n,m}(\mathbf{x}) \right. \\
& \quad \left. - (n+m) \int d_K^2(D_{\mathcal{Y}}, D_{G_m}) dH_{n,m}(\mathbf{x}) > t_{1-\alpha}^{(2)} \right\} \\
& \geq \mathbb{P}_{F_n, G_m} \left\{ (n+m) \int d_K^2(D_{\mathcal{X}}, D_{F_n}) dH_{n,m}(\mathbf{x}) \right. \\
& \quad \left. + (n+m) \int d_K^2(D_{\mathcal{Y}}, D_{G_m}) dH_{n,m}(\mathbf{x}) \leq \int \Delta_{n,m}^2 d\mathbf{x} - t_{1-\alpha}^{(2)} \right\} \\
& \rightarrow 1 \text{ as } \min(n, m) \rightarrow \infty. \tag{29}
\end{aligned}$$

The last implication follows from the same facts that are used in Equation (28). \square

Proof of Theorem 8.

Observe that the log-likelihood ratio for testing $H_0 : F = F_0$ against H_n described in (16),

$$\begin{aligned}
\mathcal{L}_n &= \sum_{i=1}^n \log \frac{(1 - \gamma/\sqrt{n}) f_0(\mathbf{x}_i) + (\gamma/\sqrt{n}) h(\mathbf{x}_i)}{f_0(\mathbf{x}_i)} \\
&= \sum_{i=1}^n \log \left\{ 1 + (\gamma/\sqrt{n}) \left[\frac{h(\mathbf{x}_i)}{f_0(\mathbf{x}_i)} - 1 \right] \right\} \\
&= \frac{\gamma}{\sqrt{n}} \sum_{i=1}^n \left\{ \frac{h(\mathbf{x}_i)}{f_0(\mathbf{x}_i)} - 1 \right\} - \frac{\gamma^2}{2n} \sum_{i=1}^n \left\{ \frac{h(\mathbf{x}_i)}{f_0(\mathbf{x}_i)} - 1 \right\}^2 + \mathcal{R}_n \\
&= \frac{\gamma}{\sqrt{n}} \sum_{i=1}^n \mathcal{K}_i - \frac{\gamma^2}{2n} \sum_{i=1}^n \mathcal{K}_i^2 + \mathcal{R}_n \tag{30}
\end{aligned}$$

where $\mathcal{K}_i = \frac{h(\mathbf{x}_i)}{f_0(\mathbf{x}_i)} - 1$. Since $\sigma^2 = \mathbb{E}_{F_0} \left\{ \frac{h(\mathbf{x})}{f_0(\mathbf{x})} - 1 \right\}^2$ is finite, $\mathcal{R}_n \xrightarrow{\mathbb{P}} 0$ as $n \rightarrow \infty$. Contiguity of the sequence H_n directly follows from Dhar et al. (2014) (see Theorem 6.1) since the first term of Equation (30) is asymptotically normal with mean zero and variance $\gamma^2 \sigma^2$ due to central limit theorem and second term converges in probability

to $\gamma^2\sigma^2/2$ due to weak law of large numbers. Therefore, by Slutsky's theorem, \mathcal{L}_n is asymptotically normal with mean $-\gamma^2\sigma^2/2$ and variance $\gamma^2\sigma^2$. An application of Le Cam's first lemma, we can deduce the first part of the theorem.

Now, to apply Le Cam's third lemma, we need to calculate the covariance between $D_{\mathcal{X}} - D_{F_0}$ and \mathcal{L}_n under null.

Let $\mathcal{T}(F)$ be a functional defined for all distributions in a stable class, then the influence function of \mathcal{T} at F is defined as $\text{IF}(\mathbf{z}; \mathcal{T}(F)) = \lim_{\epsilon \rightarrow 0^+} \frac{\mathcal{T}((1-\epsilon)F + \epsilon\delta_{\mathbf{z}}) - \mathcal{T}(F)}{\epsilon}$ where $\delta_{\mathbf{z}}$ is the point mass probability measure at $\mathbf{z} \in \mathbb{R}^d$ and $\epsilon \in [0, 1]$. For any $\mathbf{z} \in \mathbb{R}^d$, partition the set closed half-space \mathcal{H} as $\mathcal{H}_{\mathbf{z}} = \{H \in \mathcal{H} : \mathbf{z} \in H\}$ and $\mathcal{H}_{\bar{\mathbf{z}}} = \{H \in \mathcal{H} : \mathbf{z} \notin H\}$. Thus, corresponding depths are defined as $D_F^{\mathbf{z}}(\mathbf{x}) = \inf_{\mathcal{H}_{\mathbf{z}}} F(H)$ and $D_F^{\bar{\mathbf{z}}}(\mathbf{x}) = \inf_{\mathcal{H}_{\bar{\mathbf{z}}}} F(H)$ respectively. Then the influence function of half-space depth becomes $\text{IF}(\mathbf{z}; D_F(\mathbf{x})) = -D_F(\mathbf{x})\mathbf{1}\{D_F^{\bar{\mathbf{z}}}(\mathbf{x}) < D_F^{\mathbf{z}}(\mathbf{x})\} + (1 - D_F(\mathbf{x}))\mathbf{1}\{D_F^{\bar{\mathbf{z}}}(\mathbf{x}) \geq D_F^{\mathbf{z}}(\mathbf{x})\}$ (Romanazzi, 2001), where $\mathbf{1}\{a \in A\}$ takes value 1 if $a \in A$ and zero otherwise. If $\mathbf{z} = \mathbf{x}$, then, $\mathcal{H}_{\mathbf{z}} = \mathcal{H}$ and $\mathcal{H}_{\bar{\mathbf{z}}}$ becomes null-set. Hence $\text{IF}(\mathbf{x}; D_F(\mathbf{x})) = 1 - D_F(\mathbf{x})$. Note that, IF is bounded, and is a step function. For all \mathbf{x} belonging to optimal half-space $\text{IF}(\mathbf{z}; D_{F_0}(\mathbf{x}))$ is constant and equal to $1 - D_F(\mathbf{x})$ and for all \mathbf{z} belonging to non-optimal half-spaces, $\text{IF}(\mathbf{z}; D_{F_0}(\mathbf{x}))$ is constant and equal to $D_F(\mathbf{x})$. Since by the assumption optimal half-space depth associated to \mathbf{x} is unique, then for suitable regularity conditions on F_0 (Serfling, 2009) we can write the von-Mises expansion (Romanazzi, 2001) as

$$D_{\mathcal{X}}(\mathbf{x}) - D_{F_0}(\mathbf{x}) = \frac{1}{n} \sum_{i=1}^n \text{IF}(\mathbf{X}_i; D_{F_0}(\mathbf{x})) + \mathcal{E}_n \quad (31)$$

where \mathcal{E}_n is the remaining term. Due to central limit theorem, it can be shown that $\sqrt{n}\mathcal{E}_n \xrightarrow{\mathbb{P}} 0$ (see Appendix 2 of Romanazzi (2001)). Therefore, the asymptotic covariance function between $\sqrt{n}(D_{\mathcal{X}}(\mathbf{x}) - D_{F_0}(\mathbf{x}))$ and \mathcal{L}_n is

$$\begin{aligned} & \text{cov}_{H_0} \left\{ \sqrt{n}(D_{\mathcal{X}}(\mathbf{x}) - D_{F_0}(\mathbf{x})), \mathcal{L}_n \right\} \\ &= \frac{\gamma}{n} \text{cov}_{H_0} \left\{ \sum_{i=1}^n \text{IF}(\mathbf{X}_i; D_{F_0}(\mathbf{x})), \sum_{i=1}^n \mathcal{K}_i \right\} - \frac{\gamma^2}{2n^{3/2}} \text{cov}_{H_0} \left\{ \sum_{i=1}^n \text{IF}(\mathbf{X}_i; D_{F_0}(\mathbf{x})), \sum_{i=1}^n \mathcal{K}_i^2 \right\} \\ &= -\gamma \text{cov}_{H_0} \left\{ D_{F_0}(\mathbf{x}), \frac{h(\mathbf{x})}{f_0(\mathbf{x})} \right\} + \frac{\gamma^2}{2\sqrt{n}} \text{cov}_{H_0} \left\{ D_{F_0}(\mathbf{x}), \left(\frac{h(\mathbf{x})}{f_0(\mathbf{x})} - 1 \right)^2 \right\} \\ &= -\gamma \int D_{F_0}(\mathbf{x}) h(\mathbf{x}) d\mathbf{x} + o(1) \end{aligned} \quad (32)$$

The last implication follows from the fact that $\text{cov}_{H_0} \left\{ D_{F_0}(\mathbf{x}), \left(\frac{h(\mathbf{x})}{f_0(\mathbf{x})} - 1 \right)^2 \right\}$ is finite that can be shown by applying Cauchy-Schwarz inequality with the fact that $\text{Var}_{H_0} \{ D_{F_0}(\mathbf{x}) \}$ and $\mathbb{E}_{H_0} \left\{ \frac{h(\mathbf{x})}{f_0(\mathbf{x})} - 1 \right\}^4$ are finite. Thus, by Le Cam's third lemma, under contiguous alternatives the empirical Tukey's half-space depth process i.e. $\sqrt{n}(D_{\mathcal{X}}(\mathbf{x}) - D_{F_0}(\mathbf{x}))$ converges to \mathcal{G}'_1 which is Gaussian process with mean $-\gamma \mathbb{E}_{\mathbf{x} \sim h} \{ D_{F_0}(\mathbf{x}) \}$ and the covariance kernel $F_0(H[\mathbf{x}_1] \cap H[\mathbf{x}_2]) - F_0(H[\mathbf{x}_1])F_0(H[\mathbf{x}_2])$. Moreover, $\sqrt{n}(D_{\mathcal{X}}(\mathbf{x}) - D_{F_0}(\mathbf{x}))$ satisfies the tightness condition under contiguous alternatives since it is tight under null. The tightness under null follows from the weak convergence of the empirical Tukey's depth process (see Proposition 4). Therefore, by Le Cam's third lemma, under the contiguous alternatives alternatives H_n , the asymptotic power of the test based on $T_{\mathcal{X}, F_0}^{\text{KS}}$ and $T_{\mathcal{X}, F_0}^{\text{CvM}}$ are $\mathbb{P}_\gamma \left\{ \sup_{\mathbf{x}} |\mathcal{G}'_1(\mathbf{x})| > s_{1-\alpha}^{(1)} \right\}$ and $\mathbb{P}_\gamma \left\{ \int |\mathcal{G}'_1(\mathbf{x})|^2 dF_0(\mathbf{x}) > s_{1-\alpha}^{(2)} \right\}$, respectively. \square

Proof of Theorem 8. Observe that the likelihood ratio for testing $H_0 : F = G$ against $H_{n,m}$ described in (17),

$$\begin{aligned}
\mathcal{L}_{n,m} &= \sum_{i=1}^n \sum_{j=1}^m \log \frac{f(\mathbf{x}_i) \left\{ (1 - \gamma/\sqrt{n+m})f(y_j) + \gamma h(\mathbf{y}_j)/\sqrt{n+m} \right\}}{f(\mathbf{x}_i)f(\mathbf{y}_i)} \\
&= \sum_{j=1}^m \log \left\{ 1 + \frac{\gamma}{\sqrt{n+m}} \left(\frac{h(y_j)}{f(y_j)} - 1 \right) \right\} \\
&= \frac{\gamma}{\sqrt{n+m}} \sum_{j=1}^m \left\{ \frac{h(\mathbf{y}_j)}{f(\mathbf{y}_j)} - 1 \right\} - \frac{\gamma^2}{2(n+m)} \sum_{j=1}^m \left\{ \frac{h(\mathbf{y}_j)}{f(\mathbf{y}_j)} - 1 \right\}^2 + \mathcal{R}_{n,m} \\
&= \frac{\gamma}{\sqrt{n+m}} \sum_{j=1}^m \mathcal{K}'_j - \frac{\gamma^2}{2(n+m)} \sum_{j=1}^m \mathcal{K}'_j^2 + \mathcal{R}_{n,m}
\end{aligned} \tag{33}$$

where $\mathcal{K}'_i = \frac{h(\mathbf{y}_j)}{f(\mathbf{y}_j)} - 1$. Since $\sigma^2 = \mathbb{E} \left\{ \frac{h(\mathbf{y})}{f(\mathbf{y})} - 1 \right\}^2$ is finite, $\mathcal{R}_{n,m} \xrightarrow{\mathbb{P}} 0$ as $\min(n, m) \rightarrow \infty$. Contiguity of the sequence $H_{n,m}$ directly follows from Dhar et al. (2014) (see Theorem 6.2) since the first term of Equation (33) is asymptotically normal with mean zero and variance $\gamma^2 \sigma^2 (1 - \lambda)$ due to central limit theorem and second term converges in probability to $-\gamma^2 \sigma^2 (1 - \lambda)/2$. Therefore, by Slutsky's theorem, $\mathcal{L}_{n,m}$ is asymptotically normal with mean $-\gamma^2 \sigma^2 (1 - \lambda)/2$ and variance $\gamma^2 \sigma^2 (1 - \lambda)$. An application of Le Cam's first lemma, we can deduce the first part of the theorem.

Now, to apply Le Cam's third lemma, we need to calculate the covariance between

$D_{\mathcal{X}} - D_{\mathcal{Y}}$ and $\mathcal{L}_{n,m}$ under null. As in the proof of Theorem 8, using von-Mises expansion described in Equation (31) and the fact that \mathcal{X} and \mathcal{Y} are independent, we have

$$\begin{aligned}
& \text{cov}_{H_0} \left\{ \sqrt{n+m} (D_{\mathcal{X}}(\mathbf{u}) - D_{\mathcal{Y}}(\mathbf{u})), \mathcal{L}_{n,m} \right\} \\
&= \gamma \text{cov}_{H_0} \left\{ \sqrt{n+m} (D_{\mathcal{X}}(\mathbf{u}) - D_{\mathcal{Y}}(\mathbf{u})), \frac{1}{\sqrt{n+m}} \sum_{j=1}^m \mathcal{K}'_j \right\} \\
&\quad - \frac{\gamma^2}{2} \text{cov}_{H_0} \left\{ \sqrt{n+m} (D_{\mathcal{X}}(\mathbf{u}) - D_{\mathcal{Y}}(\mathbf{u})), \frac{1}{(n+m)} \sum_{j=1}^m \mathcal{K}'_j^2 \right\} := \gamma \mathcal{A}_1 - \frac{\gamma^2}{2} \mathcal{A}_2
\end{aligned} \tag{34}$$

where

$$\begin{aligned}
\mathcal{A}_1 &= \text{cov}_{H_0} \left\{ \sqrt{n+m} (D_{\mathcal{X}}(\mathbf{u}) - D_{\mathcal{Y}}(\mathbf{u})), \frac{1}{\sqrt{n+m}} \sum_{j=1}^m \mathcal{K}'_j \right\} \\
&= -\text{cov}_{H_0} \left\{ (1-\lambda)^{-1/2} \sqrt{m} (D_{\mathcal{Y}}(\mathbf{u}) - D_F(\mathbf{u})), \frac{1}{\sqrt{n+m}} \sum_{j=1}^m \mathcal{K}'_j \right\} \\
&= -(1-\lambda)^{-1/2} \text{cov}_{H_0} \left\{ \frac{1}{\sqrt{m}} \sum_{j=1}^m \text{IF}(\mathbf{y}_j; D_F(\mathbf{u})), \frac{1}{\sqrt{n+m}} \sum_{j=1}^m \mathcal{K}'_j \right\} \\
&= \sqrt{\frac{\lambda}{1-\lambda}} \text{cov}_{H_0} \left\{ D_F(\mathbf{u}), \frac{h(\mathbf{u})}{f(\mathbf{u})} \right\} = \sqrt{\frac{\lambda}{1-\lambda}} \int D_F(\mathbf{u}) h(\mathbf{u}) d\mathbf{u}
\end{aligned} \tag{35}$$

and similar to the second term of Equation (32), under the condition $\mathbb{E} \left\{ \frac{h(\mathbf{x})}{f(\mathbf{x})} - 1 \right\}^4 < \infty$, by applying Cauchy-Schwarz inequality, $\mathcal{A}_2 = o(1)$ as $\min(n, m) \rightarrow \infty$. Thus, the covariance between $\sqrt{n+m} (D_{\mathcal{X}}(\mathbf{u}) - D_{\mathcal{Y}}(\mathbf{u}))$ and $\mathcal{L}_{n,m}$ is $\gamma \sqrt{\lambda/(1-\lambda)} \mathbb{E}_{\mathbf{u} \sim h} \{ D_F(\mathbf{u}) \}$.

Thus, by Le Cam's third lemma, under contiguous alternatives the empirical Tukey's half-space depth process i.e. $\sqrt{n+m} (D_{\mathcal{X}}(\mathbf{u}) - D_{\mathcal{Y}}(\mathbf{u}))$ converges to \mathcal{G}'_2 which is Gaussian process with mean $\gamma \sqrt{\lambda/(1-\lambda)} \mathbb{E}_{\mathbf{u} \sim h} \{ D_F(\mathbf{u}) \}$ and the covariance kernel $\{ F(H[\mathbf{u}_1] \cap H[\mathbf{u}_2]) - F(H[\mathbf{u}_1]) F_0(H[\mathbf{u}_2]) \} / \lambda(1-\lambda)$. Moreover, $\sqrt{n+m} (D_{\mathcal{X}}(\mathbf{u}) - D_{\mathcal{Y}}(\mathbf{u}))$ satisfies the tightness condition under contiguous alternatives since it is tight under null. The tightness under null follows from the weak convergence of the empirical Tukey's depth process (under the independence of \mathcal{X} and \mathcal{Y} , for $\lambda \in (0, 1)$, see Proposition 4). Therefore, by Le Cam's third lemma, under the contiguous alternatives alternatives H_n , the asymptotic power of the test based

on $T_{\mathcal{X},\mathcal{Y}}^{\text{KS}}$ and $T_{\mathcal{X},\mathcal{Y}}^{\text{CvM}}$ are $\mathbb{P}_\gamma \left\{ \sup_{\mathbf{u}} |\mathcal{G}'_2(\mathbf{u})| > t_{1-\alpha}^{(1)} \right\}$ and $\mathbb{P}_\gamma \left\{ \int |\mathcal{G}'_2(\mathbf{u})|^2 dH_{n,m}(\mathbf{u}) > t_{1-\alpha}^{(2)} \right\}$, respectively. \square

References

Anderson, T. W. (1962). On the distribution of the two-sample cramer-von mises criterion. *The Annals of Mathematical Statistics*, 1148–1159.

Anderson, T. W. and D. A. Darling (1952). Asymptotic theory of certain” goodness of fit” criteria based on stochastic processes. *The annals of mathematical statistics*, 193–212.

Azzalini, A. and A. D. Valle (1996). The multivariate skew-normal distribution. *Biometrika* 83(4), 715–726.

Brown, B. M. and T. P. Hettmansperger (1989). An affine invariant bivariate version of the sign test. *Journal of the Royal Statistical Society: Series B (Methodological)* 51(1), 117–125.

Chambers, J. M., W. S. Cleveland, B. Kleiner, and P. A. Tukey (2018). *Graphical methods for data analysis*. Chapman and Hall/CRC.

Chen, H. and J. H. Friedman (2017). A new graph-based two-sample test for multivariate and object data. *Journal of the American statistical association* 112(517), 397–409.

Cuesta-Albertos, J. and A. Nieto-Reyes (2008). The tukey and the random tukey depths characterize discrete distributions. *Journal of Multivariate Analysis* 99(10), 2304 – 2311.

Daniel, W. W. (1990). Kolmogorov–smirnov one-sample test. *Applied nonparametric statistics* 2.

Dhar, S. S., B. Chakraborty, and P. Chaudhuri (2014). Comparison of multivariate distributions using quantile–quantile plots and related tests. *Bernoulli* 20(3), 1484–1506.

Donoho, D. L. and M. Gasko (1992). Breakdown properties of location estimates based on halfspace depth and projected outlyingness. *The Annals of Statistics*, 1803–1827.

Doornik, J. A. and H. Hansen (2008). An omnibus test for univariate and multivariate normality. *Oxford bulletin of economics and statistics* 70, 927–939.

Efron, B. (1982). *The jackknife, the bootstrap and other resampling plans*. SIAM.

Friedman, J. H. and L. C. Rafsky (1981). Graphics for the multivariate two-sample problem. *Journal of the American Statistical Association* 76(374), 277–287.

Gnanadesikan, R. (2011). *Methods for statistical data analysis of multivariate observations*. John Wiley & Sons.

Gower, J. (1974). Algorithm as 78: The mediancentre. *Journal of the Royal Statistical Society. Series C (Applied Statistics)* 23(3), 466–470.

Hassairi, A. and O. Regaieg (2008). On the tukey depth of a continuous probability distribution. *Statistics & probability letters* 78(15), 2308–2313.

Henze, N. and B. Zirkler (1990). A class of invariant consistent tests for multivariate normality. *Communications in statistics-Theory and Methods* 19(10), 3595–3617.

Hodges, J. L. (1955). A bivariate sign test. *The Annals of Mathematical Statistics* 26(3), 523–527.

Kong, L. and Y. Zuo (2010). Smooth depth contours characterize the underlying distribution. *Journal of Multivariate Analysis* 101(9), 2222 – 2226.

Koshevoy, G. A. (2002). The tukey depth characterizes the atomic measure. *Journal of Multivariate Analysis* 83(2), 360–364.

Koshevoy, G. A. (2003). Lift-zonoid and multivariate depths. In *Developments in Robust Statistics*, pp. 194–202. Springer.

Koziol, J. A. (1982). A class of invariant procedures for assessing multivariate normality. *Biometrika* 69(2), 423–427.

Liu, R. (1990). Liu, on a notion of data depth based on random simplices. *Ann. Statist* 18, 405–414.

Liu, R. Y., J. M. Parelius, and K. Singh (1999). Multivariate analysis by data depth: descriptive statistics, graphics and inference, (with discussion and a rejoinder by Liu and Singh). *Ann. Statist.* 27(3), 783–858.

Lorenz, M. O. (1905). Methods of measuring the concentration of wealth. *Publications of the American Statistical Association* 9(70), 209–219.

Mahalanobis, P. C. (1936). On the generalized distance in statistics. National Institute of Science of India.

Marden, J. I. (1998). Bivariate qq-plots and spider web plots. *Statistica Sinica*, 813–826.

Marden, J. I. (2004). Positions and qq plots. *Statistical Science*, 606–614.

Massé, J.-C. (2004). Asymptotics for the Tukey depth process, with an application to a multivariate trimmed mean. *Bernoulli* 10(3), 397–419.

Michael, J. R. (1983). The stabilized probability plot. *Biometrika* 70(1), 11–17.

Mosler, K. (2013). Depth statistics. *Robustness and complex data structures*, 17–34.

Newland, R. P., S. H. Parade, S. Dickstein, and R. Seifer (2016). Goodness of fit between prenatal maternal sleep and infant sleep: Associations with maternal depression and attachment security. *Infant behavior and development* 44, 179–188.

Oja, H. (1983). Descriptive statistics for multivariate distributions. *Statistics & Probability Letters* 1(6), 327–332.

Paraschiv-Ionescu, A., E. Buchser, and K. Aminian (2013). Unraveling dynamics of human physical activity patterns in chronic pain conditions. *Scientific reports* 3(1), 1–10.

Paulson, A., P. Roohan, and P. Sullo (1987). Some empirical distribution function tests for multivariate normality. *Journal of Statistical Computation and Simulation* 28(1), 15–30.

Pollard, D. (1984). *Convergence of stochastic processes*. Springer Science & Business Media.

Romanazzi, M. (2001). Influence function of halfspace depth. *Journal of Multivariate Analysis* 77(1), 138 – 161.

Rousseeuw, P. J. and I. Ruts (1996). Algorithm as 307: Bivariate location depth. *Journal of the Royal Statistical Society. Series C (Applied Statistics)* 45(4), 516–526.

Rousseeuw, P. J. and A. Struyf (1998). Computing location depth and regression depth in higher dimensions. *Statistics and Computing* 8(3), 193–203.

Royston, P. (1992). Approximating the shapiro-wilk w-test for non-normality. *Statistics and computing* 2(3), 117–119.

Ruts, I. and P. J. Rousseeuw (1996). Computing depth contours of bivariate point clouds. *Computational Statistics & Data Analysis* 23(1), 153 – 168. Classification.

Serfling, R. J. (2009). *Approximation theorems of mathematical statistics*, Volume 162. John Wiley & Sons.

Sidak, Z., P. K. Sen, and J. Hajek (1999). *Theory of rank tests*. Academic press.

Tibshirani, R. J. and B. Efron (1993). An introduction to the bootstrap. *Monographs on statistics and applied probability* 57, 1–436.

Tukey, J. W. (1975). Mathematics and the picturing of data. In *Proceedings of the international congress of mathematicians*, Volume 2, pp. 523–531.

Voinov, V., N. Pya, R. Makarov, and Y. Voinov (2016). New invariant and consistent chi-squared type goodness-of-fit tests for multivariate normality and a related comparative simulation study. *Communications in Statistics-Theory and Methods* 45(11), 3249–3263.

Webster, R. (1977). Spectral analysis of gilgai soil. *Soil Research* 15(3), 191–204.

Wilk, M. B. and R. Gnanadesikan (1968). Probability plotting methods for the analysis for the analysis of data. *Biometrika* 55(1), 1–17.

Zuo, Y. and R. Serfling (2000). General notions of statistical depth function. *Annals of statistics*, 461–482.